

Low-mass visual companions to nearby G-dwarfs

Andrei Tokovinin

Cerro Tololo Inter-American Observatory, Casilla 603, La Serena, Chile

atokovinin@ctio.noao.edu

ABSTRACT

Complete census of wide visual companions to nearby G-dwarf stars can be achieved by selecting candidates from the 2MASS Point-Source Catalog and checking their status by second-epoch imaging. Such data are obtained for 124 candidates with separations up to $20''$, 47 of which are shown to be new physical low-mass stellar companions. A list of visual binaries with G-dwarf primaries is produced by combining newly found companions with historical data. Maximum likelihood analysis leads to the companion frequency of 0.13 ± 0.015 per decade of separation. The mass ratio is distributed almost uniformly, with a power-law index between -0.4 and 0 . The remaining uncertainty in the index is related to modeling of the companion detection threshold in 2MASS. These findings are confirmed by alternative analysis of wider companions in 2MASS, removing the contamination by background stars statistically. Extension of this work will lead to a complete detection of visual companions – a necessary step towards reaching unbiased multiplicity statistics over the full range of orbital periods and, eventually, understanding the origin of multiple systems.

Subject headings: stars: binaries

1. Introduction

Attention to low-mass stars in the solar neighborhood is mostly inspired by searches for exoplanets. Looking for stellar companions is less popular nowadays, although solid empirical data on the distribution of periods, mass ratios, and hierarchies are still much needed for understanding the origin of stars, multiple systems, and planets (Bate 2008). Even within the 25-pc distance the multiplicity statistics of G-dwarfs is still being updated and revised (Raghavan et al. 2010). An order-of-magnitude larger sample is required, however, to study detailed distributions of orbital parameters and higher-order hierarchies (triples, quadruples, etc.).

Periods of binary systems range from half-day to millions of years. Discovery of all companions over the entire parameter space requires combination of complementary techniques. Precise radial velocities cover periods up to few years, but information at longer periods is still dominated by visual discoveries over the last two centuries.

These data, collected in the Washington Double Star Catalog, WDS (Mason et al. 2001), are notoriously incomplete, especially for low-mass companions.

The Two Micron All-Sky Survey, 2MASS (Cutri et al. 2003) covers the whole sky in the JHK_s near-IR bands. Its sensitivity is sufficient for detecting even a $0.08-M_\odot$ companion to a G-dwarf star at 60 pc. The problem is in separating true (*physical*) companions from the background stars (*optical* companions). At large separations, physical companions can be identified by their common proper motion (PM) (Lépine & Bongiorno 2007; Makarov, Zacharias, & Hennessy 2008). However, the PM data are mostly based on archival photographic images where the vicinity of bright primary stars is contaminated by their halo, preventing detection of very faint companions (the magnitude difference in the visible is larger than in the IR). Meanwhile, physical companions should dominate over background interlopers at small separations. IR imaging is

used to find visual companions to exoplanet host stars by, e.g. Mugrauer & Neuhäuser (2009). Kirkpatrick et al. (2010) took second-epoch images of 10% of sky and found many new common-proper-motion companions by comparison with the 2MASS.

The purpose of this work is to explore the potential of 2MASS for reaching a complete census of stellar companions to nearby dwarfs with separations from a few arcseconds to $20'' - 30''$. At smaller separations, adaptive-optics imaging (Shatsky & Tokovinin 2002; Kraus et al. 2008; Metchev & Hillenbrandt 2009; Chauvin et al. 2010) can be used, at larger separations the existing PM data may be sufficient. I take second-epoch images of carefully selected companion candidates from the 2MASS Point-Source Catalog (hereafter PSC) (Cutri et al. 2003) to determine their status (physical or optical). The detection limit of the PSC is modeled. The data set on visual companions in the selected range of separations is complemented by the new discoveries from 2MASS and used to study the distribution of the companion mass ratio, $f(q)$. I show that $f(q)$ is approximately uniform. This refers to wide binaries studied here; a typical $10''$ binary at 60 pc distance has semi-major axis of 600 AU and an orbital period on the order of 15 000 yr.

New companions to G-dwarfs found here extend their number by 55%, complementing the census in the low-mass regime. About 1/3 of the new binaries are higher-order multiples. More companion candidates from the PSC wait to be confirmed by contemporary imaging. This study thus contributes to a larger task of obtaining unbiased multiplicity statistics of nearby G-dwarfs.

The sample of nearby G-dwarfs and criteria for selecting candidate companions are presented in Section 2. Section 3 describes the observations and their processing. The results are presented in Section 4, followed by the statistical analysis in Section 5. The paper closes by discussion in Section 6.

2. The sample

The targets chosen for this survey belong to a large sample of nearby solar-type dwarfs (*Nsample*) selected from the *Hipparcos* catalog (ESA 1997) in its latest version (van Leeuwen 2007) by

the following criteria.

1. Trigonometric parallax $\pi_{\text{HIP}} < 15$ mas (within 67 pc from the Sun, distance modulus $< 4.12^m$).
2. Color $0.5 < V - I < 0.8$ (this corresponds approximately to spectral types from F5V to K0V).
3. Unevolved, satisfying the condition $M_{\text{HP}} > 9(V - I) - 3.5$, where M_{HP} is the absolute magnitude in the *Hipparcos* band calculated with π_{HIP} .

There are 5040 catalog entries satisfying these conditions. The selection criteria may introduce some bias with respect to unresolved binaries, to be addressed in the final statistics but irrelevant for the present study. Systems containing white dwarfs should be removed from the statistics, as the present-day G-dwarfs are not original primaries. Removal of the secondary components of binaries with separate HIP numbers and 6 stars with parallax errors larger than 7.5 mas leaves 4915 primary targets. This sample includes many stars monitored for exoplanets and young stars in the solar neighbourhood (X-ray sources, members of T-associations).

All point sources within $2.5'$ radius from each target are extracted from the PSC. The number of companions around each target, N^* , varies strongly and is a good measure of crowding. The total number of stars around primaries is 114404, or $N^* = 23.3$ on average. Most of these companions are faint.

Trying to isolate potential physical companions, I consider only point sources within $20''$ from primary targets which do not belong to crowded fields, $N^* < 100$. Primary components not found in 2MASS (within $6''$) are skipped. This leaves 5347 stars, of which 4281 are primaries, 1066 are candidate secondaries. Among the secondaries, 238 are known companions listed in the WDS (Mason et al. 2001).

Observations were conducted to determine which of the companions are physical. New imaging covers the right ascension zone from 2^h to 18^h and declinations south of $+20^\circ$, 0.447 fraction of the whole sky. As the majority of the candidate companions are too faint to be on the

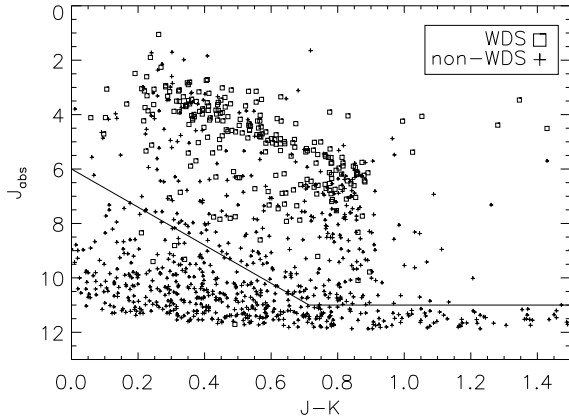


Fig. 1.— The $(J_{\text{abs}}, J-K)$ CMD of PSC candidate companions within $20''$ from the N_{sample} targets.

Main-Sequence (MS), an additional selection criterion is imposed,

$$J_{\text{abs}} < 6 + 7(J - K) \quad \text{and} \quad J_{\text{abs}} < 11. \quad (1)$$

Thus, 366 potential companions are above the solid line on the $(J_{\text{abs}}, J-K)$ color-magnitude diagram (CMD) in Fig. 1, constructed by assigning the parallaxes of primary targets to their companion candidates. The selection criterion is intentionally “soft” because some physical companions are known to deviate from the MS (see discussion of Hipparcos dwarfs with deviant colors in Koen et al. 2010). The nature of companions already listed in the WDS can be established with existing data, so most of them were dropped from the observing program, leaving 136 targets in the list. However, known companions are included in the statistical analysis.

3. Observations and data reduction

3.1. Imaging data

Simultaneous images in the visible and IR were taken at the CTIO 1.3-m telescope (the telescope used in the 2MASS survey) with the ANDICAM instrument¹ (DePoy et al. 2003). The visual channel has a CCD with 1024^2 binned pixels of $0''.369$ size, the IR channel has 512^2 binned pixels of $0''.274$.

¹<http://www.astronomy.ohio-state.edu/ANDICAM/detectors.html>

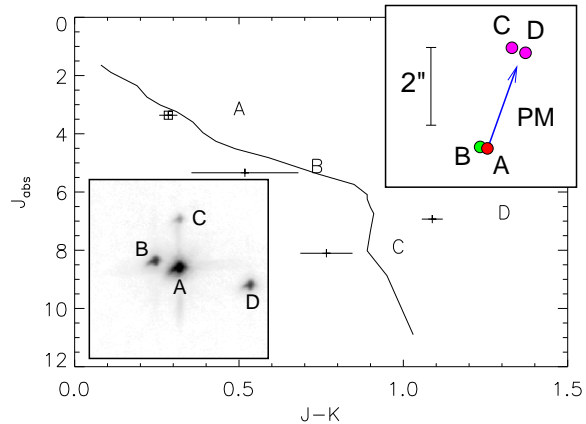


Fig. 2.— Example of the data and their interpretation. There are 3 PSC companions around HIP 25662 with separations from $5''.5$ to $16''.9$, labeled B, C, and D respectively. The location of these companions on the $(J_{\text{abs}}, J-K)$ CMD is shown. The lower-left insert is a fragment of the combined K_s image with 4-s exposure. The upper-right insert shows the displacement of the companions B, C, D relative to their PSC positions and the displacement produced by the proper motion in 10 years (arrow). The companion B is physical, C and D are optical.

Observations were carried out in February–March 2010 (2010.09 to 2010.19), in service mode. Five 4-s images of each target were taken in the K_s band with dithers of 40 pixels ($\sim 11''.6$), followed by five 30-s dithered images. Simultaneously, several V-band images with 2-s and 30-s exposures were recorded. Most results reported here were obtained from the short-exposure images.

There are several problems in the data. HIP 10710 was not pointed correctly, HIP 59250, 60155, 60251, 60337, 61298, 61608, 73764 were not observed at all. For 7 other targets (HIP 41620, 44579, 44777, 47312, 52676, 54285, 75839) the short-exposure sequence was not executed, leaving only 30-s exposures. The median image quality (full-width at half maximum from Gaussian fits) is $0''.9$ in the K-band and $1''.1$ in the V-band, 50% of the data is within $\pm 10\%$ from the median image size. Some images are elongated, especially in the K-band (25% have ellipticity larger than 0.27).

Reduced images were retrieved from the SMARTS data center at the Yale University (the CCD im-

ages are bias-subtracted and corrected for flat field). Dithered IR images were combined in the standard way. The sky image was calculated as a median over dithered frames. Then each sky-subtracted frame was shifted to match the first frame (the shift was determined by cross-correlation). The re-centered frames were then median-combined. Figure 2 contains an example of the combined K_s image with 3 companions around HIP 25662, one of which is physical. This star has a known CPM companion LDS 6186 at $99''.4$ and is a spectroscopic binary with 3.9y period (Vogt et al. 2002). The newly found companion makes this system at least quadruple.

3.2. Relative astrometry and photometry

Accurate relative positions and intensity ratios were determined by fitting the secondary companion image with the Point-Spread Function (PSF) of the primary. Additional freedom to treat difficult cases (blended or slightly saturated images) is provided by the choice of the inner and outer radii for the fits. Usually the inner radius is zero, the outer one is 6 pixels. Even for saturated images, the fits recover relative coordinates quite well and give under-estimated, but still useful magnitude differences. The results are stable against changes in the fit radius. For close companions, the PSFs overlap, leading to under-estimation of the magnitude difference Δm and over-estimation of the separation ρ .

Astrometric calibration of two CCD frames (crowded fields around HIP 76572 and 36414) was done by J. Subasavage by referencing them to the PSC. He found the pixel scale of $0''.3715$ and angular offset of 1.5° (to be added to the measured angles). The K_s frames were calibrated by comparing the relative companion positions with the V -band measurements. The nominal pixel scale of $0''.274$ is confirmed, -2.3° has to be added to the position angles measured in the IR images. Using these calibration parameters, I find for 22 pairs with $\Delta V < 4$ the average difference $\langle \theta_V - \theta_K \rangle = 0.02^\circ \pm 0.3^\circ$. The rms scatter between V and K_s positions is $0''.26$ in separation and 1.2° in position angle. These numbers estimate the measurement errors, dominated by systematic effects rather than by the random noise.

Figure 3 compares our differential photometry in the K_s band with the PSC photometry for sep-

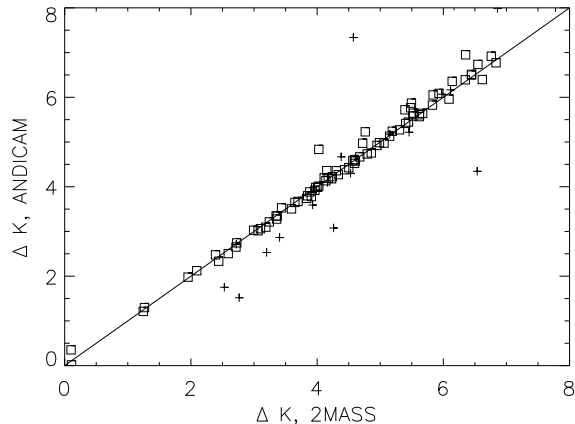


Fig. 3.— Comparison of magnitude differences in the K_s band listed in the PSC with those measured by ANDICAM for $\rho > 8''$. The 80 good-quality points (unsaturated, PSC quality flag A) are plotted as squares, the remaining 22 points as crosses.

arations $\rho > 8''$. There are only 12 cases where the two ΔK measures differ by more than 0.5^m ; the robust estimate of the rms difference is 0.095^m .

Relative astrometry and photometry of candidate binaries is listed in Table 1. It contains the *Hipparcos* number and pair identification. Then follow the separation ρ , position angle θ and magnitude difference ΔK_s derived from the PSC, with the PSC quality flag Q for the K -band photometry (Cutri et al. 2003). The remaining columns give $(\rho, \theta, \Delta m)$ measured in 2010.14 with ANDICAM in the K_s and V bands. Cases where primary components were saturated are marked by the flag S. For the most part, I use measurements from the short-exposure images.

3.3. New sub-systems?

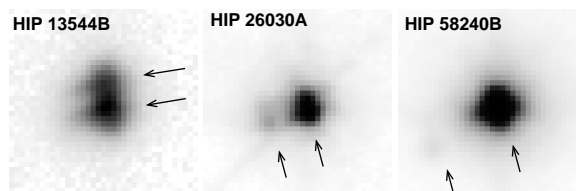


Fig. 4.— Mosaic of three partially resolved pairs in K_s band. Each square is $10''$ across, North is up and East left.

Some objects in the ANDICAM images are resolved close pairs. I do not discuss such pairs for optical companions and show in Fig. 4 only three most obvious cases of resolved physical companions. Measurements of the relative positions and magnitude differences in these close pairs are only approximate because the PSFs overlap.

HIP 13544BC is a known pair A 2341, making a triple system together with the main target. ANDICAM resolves BC into nearly equal stars at $1''.3$, 4° , $\Delta K \sim 0.6$.

HIP 26030A has a faint satellite at $1''.6$, 91° , $\Delta K = 2.7$. The new companion could be optical because this field is crowded, $N^* = 57$; there are 4 other stars in the *K*-band ANDICAM images and many more in the CCD frames.

HIP 58240B is in fact a pair Ba,Bb with parameters $3''.6$, 116° , $\Delta K = 5.8$. Further observations will help to determine the status of this pair in a moderately crowded field with $N^* = 34$.

4. Results

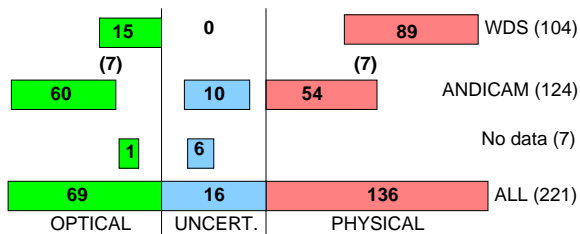


Fig. 5.— Distribution of companions over various categories.

The sample of binary stars is assembled by merging companions found in the PSC with existing data from the WDS in the same part of the sky (RA from 2^h to 18^h , $\delta < +20^\circ$). The separation of WDS companions considered here is from $5''$ to $20''$, although closer companions found in the PSC are included in the sample as well. The WDS binaries in crowded fields ($N^* > 100$) are excluded to avoid statistical bias. These selection criteria are satisfied for 1913 primary stars in the *Nsample*. I ignore 18 WDS companions not detected by the PSC for various reasons (e.g. primary component too bright or partially resolved) and exclude 15 PSC companions which are likely artifacts (not detected in all bands by 2MASS or not confirmed

here). There are 221 binary companions or candidates remaining.

All companions are classified into three groups: true (physical), background stars (optical), and uncertain. Three criteria are used.

1. Astrometry, i.e. constancy of the relative companion position over time. For the known pairs, the first-epoch positions are taken from the WDS, the last-epoch from the PSC. The new candidate binaries are checked by comparing the PSC positions with the second-epoch 2010 data. The change of the relative position is compared to the reflected PM of the primary component (Fig. 2).
2. Companion location in the $(J_{\text{abs}}, J - K)$ CMD with respect to the MS line (Lang 1992), using the distance modulus based on π_{HIP} . The photometry comes from the PSC.
3. Companion location in the $(K_{\text{abs}}, V - K)$ CMD. The *V*-magnitudes are taken from the WDS for known pairs or determined from the ΔV measured here for candidate companions detected in the *V*-band.

If random and systematic errors of the data used in these criteria were known, the formal probability of passing the tests could be computed. However, such a formal approach makes little sense for various reasons. The astrometric criterion (1) is affected by the orbital motion in the wide binaries, by motions of the components caused by un-detected inner sub-systems, and, mostly, by the unknown PMs of the background stars. In many instances the available astrometry allows a clear distinction between optical and physical companions (Fig. 2), but there remain marginal cases, especially for targets with small PM and 10-year time coverage. Similarly, the application of the criteria (2) and (3) is affected by errors in the photometry and by the possibility of physical companions being located off the MS.

I evaluated each of the 3 criteria subjectively on a continuous scale, assigning negative values for optical companions and positive values for physical ones. Larger absolute numbers mean stronger evidence, zero stands for a complete lack of infor-

mation. The combination of all 3 criteria is resumed in the opticity flag O , with -2 and -1 for certain or almost certain optical companions, $+1$ and $+2$ for very likely and certain physical companions.

Figure 5 presents the distribution of companions over the three categories (optical, uncertain, physical) and over the data sources (WDS, ANDICAM), indicating partial overlaps between these groups. The sample contains 136 physical companions, 47 of which are new (discovered in the PSC and confirmed with ANDICAM). This work thus increases the number of known physical companions in the ($5''$, $20''$) separation range around nearby G-dwarfs by 55%.

The results are summarized in Table 2, one line per pair. The systems are identified by the HIP numbers of their primary components (the cases where secondaries have distinct HIP numbers are indicated in the notes, Table 3). The V -magnitudes of the primary components are taken from the Tycho catalog (ESA 1997), the J and K_s magnitudes from the PSC. For each primary target I list π_{HIP} and N^* . For the secondary and tertiary components, the separation ρ and position angle θ based on the PSC are given. The V -band photometry of the known secondaries comes from the WDS, for some new candidates – from our measurements of ΔV . The flag $W=1$ is set if the companion is known (e.g. found in the WDS), flag $A=1$ means that the companion was observed with ANDICAM. The last column contains the opticity flag O . Table 2 also lists masses of the stars estimated from their absolute K magnitudes by relations of Henry & McCarthy (1993); obviously, for optical companions such estimates are meaningless.

More information (nature of the sub-systems etc.) is given in the notes (Table 3). In the following, I ignore the sub-systems, considering each component of a wide binary as a single star even when it is known to be a pair. This survey has produced 15 new multiple systems (HIP 11417, 11537, 12764, 25148, 25662, 34212, 36832, 39999, 41871, 47312, 52145, 54366, 56282, 68507, 84866). Spectroscopic companions to primary targets discovered by Nordström et al. (2004) are marked as N04 in the notes together with the range of radial velocity variation ΔRV in km/s. Astrometric binaries discovered by Makarov & Kaplan

(2005) are reported. About a third of the new wide binaries are actually higher-order multiples; Makarov, Zacharias, & Hennessy (2008) encounter a similarly high fraction of multiples, 25%, in their sample of CPM pairs. I give in the notes the PMs (in mas/yr) and V -band photometry from the NOMAD catalog (Zacharias et al. 2004a) for companions which are found there. However, the sources and errors of the PMs in NOMAD are not known, and in many instances they contradict my findings (discrepant PMs for physical companions or matching PMs for optical companions). Therefore, the information from NOMAD is ignored in deciding the companion status. The UCAC2 catalog (Zacharias et al. 2004b) is not deep enough ($R < 16$) to reach the faintest secondaries.

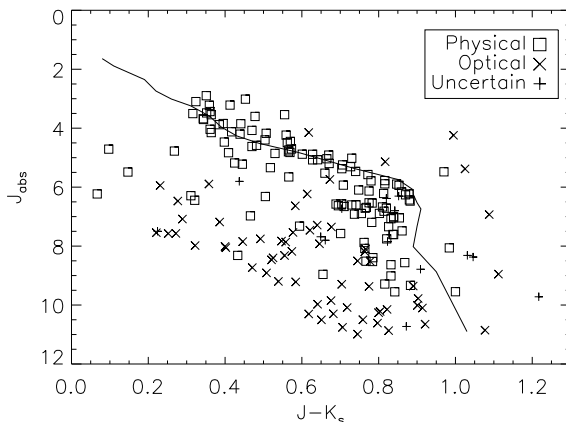


Fig. 6.— $(J_{\text{abs}}, J - K)$ CMD of the secondary companions with $\rho > 5''$. Standard MS according to Lang (1992) is shown.

Figure 6 is the $(J_{\text{abs}}, J - K)$ CMD based on the PSC photometry. Most physical companions concentrate around the MS. The spread of the points is large and there are several true companions below the MS, some of those quite bright. These outliers mostly have large photometric errors in the PSC. However, there is a real $\sim 0.2^m$ spread in the $J - K$ colors of physical companions, as follows e.g. from the work of Henry & McCarthy (1993). Most optical and uncertain companions are located below the MS. The companion selection criterion (1) leaves a convenient margin, admitting many optical candidates but not rejecting physical companions with deviant colors.

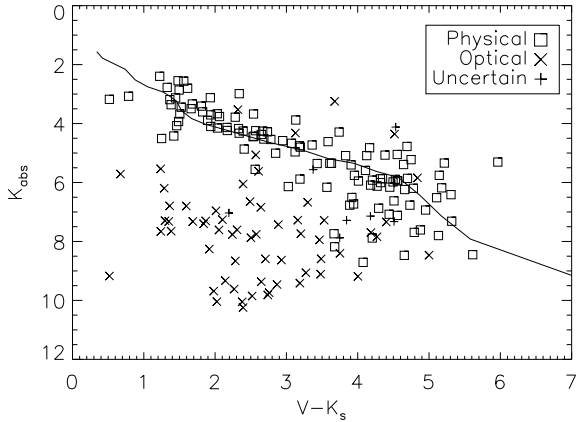


Fig. 7.— $(K_{\text{abs}}, V - K)$ CMD of the secondary companions with $\rho > 5''$. The line shows the MS.

The $(K_{\text{abs}}, V - K)$ CMD is plotted in Fig. 7. The $V - K$ color has a larger sensitivity to effective temperature, compared to $J - K$, and therefore discriminates better between physical and optical companions. The number of physical outliers is correspondingly less. However, faint and red low-mass companion candidates were not detected in the V band with ANDICAM, leaving the lower right corner of the CMD empty. Few physical companions below the MS are explained by largely under-estimated ΔV in ANDICAM images with saturated primary stars (the companions then appear bluer).

5. Statistical analysis

5.1. Detection limit in the PSC

Detection of faint sources in the PSC is complicated by the presence of nearby bright stars (primary targets). It is important to estimate this bias. Some sources are detected only in the K band, most of them are artifacts. They are, however, not removed from the candidate list, and some turn out to be genuine physical companions. For evaluating the PSC detection bias, I select companions with valid PSC photometry in all three bands JHK_s within $20''$ from the targets and plot the magnitude difference with primary components ΔK vs. separation ρ in Fig. 8. The dashed line approximates the upper envelope by two segments.

A primary target of $1 M_{\odot}$ has $K_{\text{abs}} \approx 3.1$, so the

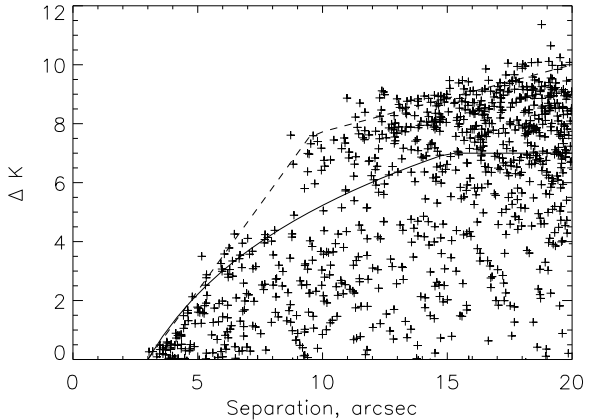


Fig. 8.— Magnitude difference ΔK vs. separation for 982 PSC companions with valid photometry. The dashed and full lines indicate the realistic and pessimistic detection thresholds, respectively.

restriction on the absolute magnitude $J_{\text{abs}} < 11$ imposed on the candidates translates to $\Delta K < 7$. The actual physical companions obey this restriction and delineate a more pessimistic threshold

$$\Delta K_{\text{lim}} = A \log_{10}(\rho/3'') \quad (2)$$

with $A = 10$ (solid line in Fig. 8). Statistical interpretation of the data depends on the adopted detection limit.

5.2. Distribution of the mass ratio

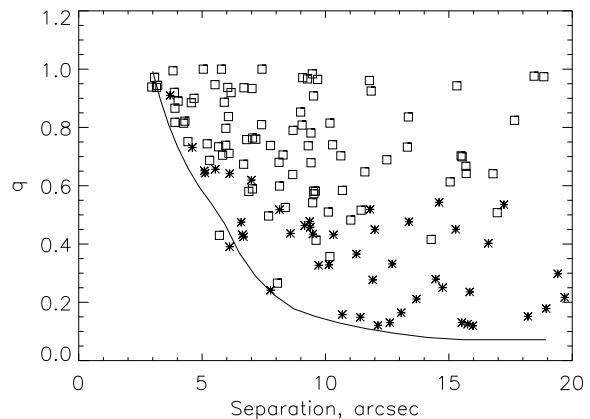


Fig. 9.— Mass ratios of binaries vs. separation. Squares – previously known systems, asterisks – new systems from the PSC. The line shows the detection limit (2) with $A = 10$.

The statistical analysis is performed on 120 physical binaries with $\rho \geq 5''$ selected by the criterion $O \geq 1$ (Table 2). Masses of the primary and secondary components, M_1 and M_2 , are estimated from their absolute magnitudes K_{abs} using the relation from (Henry & McCarthy 1993). For 3893 targets of N_{sample} common with the survey of Nordström et al. (2004) I find a good agreement with their mass estimates, to better than $\pm 10\%$. For the binaries studied here, M_1 ranges from 0.68 to $1.52 M_{\odot}$, the median M_1 is $1.03 M_{\odot}$.

Figure 9 plots the mass ratio $q = M_2/M_1$ vs. separation ρ . The estimated PSC detection limit in ΔK is translated into q assuming $M_1 = 1 M_{\odot}$. At first sight, the points are distributed uniformly in q in the space above the detection limit. There appears to be a slight preference for small q at $\rho > 12''$ and a tendency to large q at smaller separations. The actual detection limit of the PSC remains somewhat uncertain, affecting the statistical analysis. I tried several assumptions. The results reported below correspond to the hard detection limit $A = 10$, supposing that all fainter companions are missed in the PSC, all brighter ones are detected.

Considering that the companion detection “depth” is a strong function of ρ , I study the mass ratio distribution $f(q)$ for pairs with $\rho \geq \rho_{\text{min}}$, for different cutoffs ρ_{min} . The assumption is made that separations are distributed according to the Öpik’s law (constant in $\log \rho$), well established for separations around 10^3 AU (Poveda & Allen 2004). The companion frequency ϵ is normalized per decade of separation, i.e. divided by $\log(20''/\rho_{\text{min}})$, and referred to the total number of N_{sample} targets in the surveyed portion of the sky, $N = 1913$.

A power-law model of mass-ratio distribution

$$f(q) = \epsilon(\beta + 1)q^{\beta} \quad (3)$$

is frequently used in the literature (e.g. Metchev & Hillenbrand 2009). Here ϵ is the total companion fraction, β is the power index (slope). These two parameters are related because correction for the missed low-mass companions depends on β .

A histogram of the mass ratios is shown in Fig. 10. The number of companions in each bin is increased to account for incomplete detections (divided by the average detection probability in each q -bin in the separation interval $\rho_{\text{min}}, 20''$) and

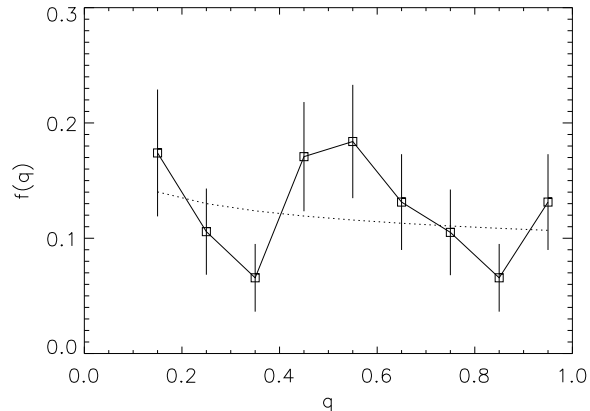


Fig. 10.— Mass-ratio histogram of 83 physical companions with $\rho > 8''$ in 0.1-wide bins, corrected for incomplete detection. The dashed line shows a power-law fit. The integral of $f(q)dq$ gives the companion frequency per decade of separation.

normalized per decade of separation. The first bin with large incompleteness is avoided, the remaining data are fitted by a line in the log-log coordinates (a power law) with $\beta = -0.15$ and $\epsilon = 0.13$. The power-law distribution describes the observed histogram adequately.

Alternatively, the model (3) can be fitted to the data directly by the maximum likelihood (ML) method, as done e.g. in (Tokovinin, Hartung, & Hayward 2010). The detection limit is included in the analysis. The likelihood function is usually interpreted as a probability distribution in the parameter space, enabling the definition of the confidence area and a better visualization of the mutual dependence between parameters (Press et al. 1992). On the other hand, the ML method requires a parametrization, in this case (3).

The results of the ML analysis depend on the assumed companion detection limit and on the separation cutoff ρ_{min} . By adopting a more strict (pessimistic) detection limit, I obtain smaller values of β and less dependence of $f(q)$ on ρ_{min} . The derived companion fraction ϵ remains nearly constant. It is expected that $f(q)$ should not depend on ρ in the relatively small interval considered here (e.g. Raghavan et al. 2010). After trying several detection limit models, I finally use a sharp threshold with $A = 10$. Please, keep in mind that the

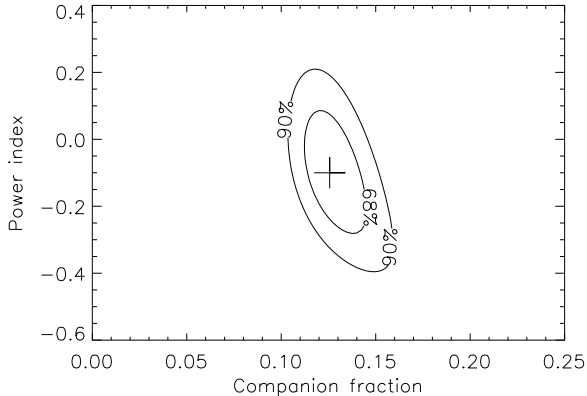


Fig. 11.— Confidence area in the (ϵ, β) parameter space for the ML solution with $\rho_{\min} = 8''$ and $A = 10$.

ML results will be somewhat different for other detection models.

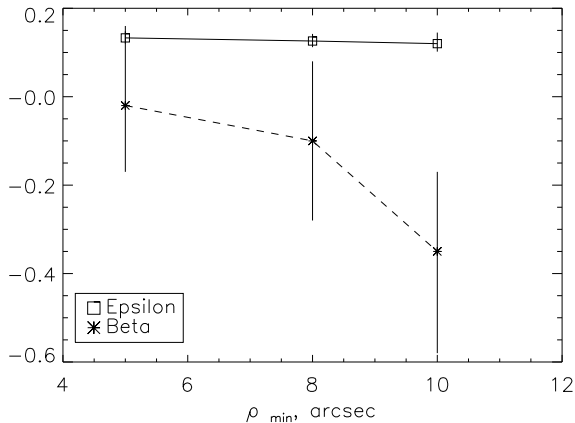


Fig. 12.— Dependence of the best-fit parameters (ϵ, β) on the ρ_{\min} for $A = 10$.

Figure 11 shows a representative result of the ML procedure for $\rho_{\min} = 8''$ (83 companions). The best-fit parameters are $\epsilon = 0.13$ and $\beta = -0.10$, the lines show the confidence areas in the parameter space corresponding to 68% (“one sigma”) and 90%. The confidence area is skewed, therefore I obtained the standard errors of parameter estimates by integrating the probability distribution over other coordinate. Figure 12 shows the dependence of the best-fit parameters and their formal $\pm\sigma$ errors on ρ_{\min} . The companion fraction ϵ is rather stable against ρ_{\min} , ranging be-

tween 0.15 and 0.13, but the power-law index β becomes more negative at larger separations, in agreement with the trend noticeable in Fig. 9.

5.3. Alternative analysis

Considering the uncertainty of the PSC detection limit for faint and close companions, I carried out an alternative analysis on wider companions between $10''$ and $30''$. This time, the PSC data over the whole sky are used. Only candidates with $J_{\text{abs}} < 11$ (bright enough to be stellar companions) and reliable PSC photometry (quality flags A–D or E in JHK_s bands) are retained. Scaling the total number of such candidates within $2.5'$ radius to the $10'' - 30''$ annulus, I expect to find 2502 and actually find 2115. There is still a small deficiency of candidates indicative of a potential detection bias. If all companions without constraints on J_{abs} are selected, the expected number is twice the actual number (10177 and 5299, respectively). Therefore, the PSC magnitude limit in the vicinity of bright stars is indeed not as deep as in the field, even at $10''$ separation.

Physical companions can be distinguished from the optical ones statistically, if not individually. To ease this task, I restrict the study to 4473 primaries where the number of stars with $J_{\text{abs}} < 11$ within $2.5'$ radius is less than 100. The CMD of the 1470 companions in the $(10'', 30'')$ separation range is shown in Fig. 13. Bright companions clearly concentrate towards the MS, merging progressively with background stars at fainter magnitudes. The separation distributions of bright and faint companions are different, the former following the Öpik’s law $f(\rho) \propto 1/\rho$ and the latter being proportional to ρ^2 .

Cumulative distributions of the $J - K$ color in four intervals of J_{abs} are plotted in Fig. 14. The vertical lines show the color range for the physical companions $0.75 < J - K < 0.9$ (P) and the comparison range $0.45 < J - K < 0.75$ (O) where only optical companions are expected. These intervals correspond to the boxes in Fig. 13. Obviously, most companions with $6 < J_{\text{abs}} < 7$ are physical, but the companion density in the ranges P and O becomes more similar and eventually equal with increasing J_{abs} . This gives a way to estimate the number of physical companions n_c in each interval

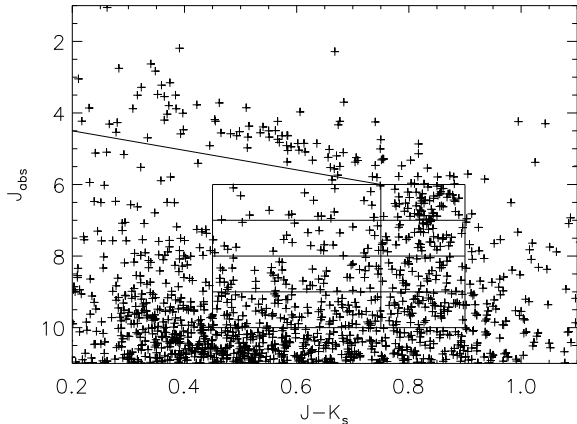


Fig. 13.— The $(J_{\text{abs}}, J - K)$ CMD of PSC companions between $10''$ and $30''$ with reliable photometry. The lines indicate box areas used for statistical analysis.

of J_{abs} as

$$n_c = n_p - 0.5n_o = \alpha n_p, \quad \alpha = 1 - n_o/(2n_p). \quad (4)$$

This formula assumes that optical companions are uniformly distributed in $J - K$, that physical companions are concentrated in the P-interval, and that the O-interval is two times larger. The contamination factor α decreases from one to nearly zero with increasing J_{abs} . The rms error of n_c estimate is, obviously, $(n_p + n_c/4)^{1/2}$. Table 4 lists the companion counts.

The fraction α of companions in the P-interval and above the tilted line in Fig. 13 are physical. Masses of the primary stars and companion candidates are estimated from their K_{abs} magnitudes using the relation from (Henry & McCarthy 1993), the mass ratios q are calculated and the distribution of q in 0.1-wide bins is constructed, applying the factors α to correct for contamination. These factors are modeled after data in Table 4 as $\alpha(q) \approx 1 - 1.5(1 - q)^4$; they become significant for $q < 0.5$, otherwise are close to 1. The last column of Table 4 gives approximate mass ratios q_0 corresponding to the centers of the J_{abs} intervals for $M_1 = 1 M_{\odot}$.

Figure 15 shows the resulting histogram. The first bin is avoided because it has a large error and a large α -correction. The values of $f(q)$ are normalized per decade of separation, assuming the Öpik's law. The dotted line shows a linear fit in

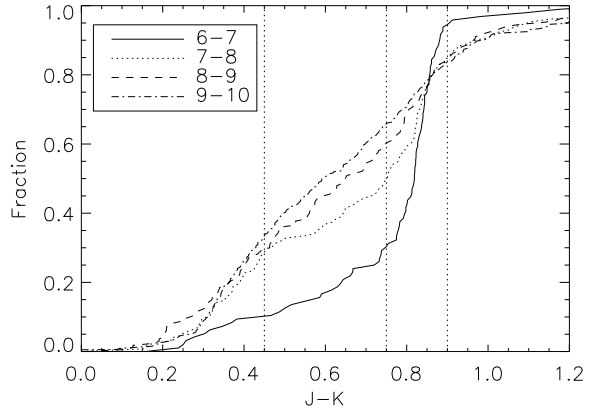


Fig. 14.— Cumulative distributions of the $J - K$ color in different intervals of J_{abs} , shown in the legend.

the log-log coordinates, i.e. a power law. The exponent is $\beta = 0.19$. The sum of $f(q)dq$ over all bins except the first one leads to $\epsilon = 0.10$.

In comparison with the histogram in Fig. 10, Fig. 15 shows a smaller fraction of low-mass companions, presumably because I do not correct here for incomplete detection. This also explains why the estimated companion fraction ϵ is slightly less than in the sub-section 5.2. However, the companions considered here are wider, hence less affected by the bright glow of the primary targets. The $f(q)$ distributions obtained by two different approaches on different (although overlapping) samples of companions are close to each other, except for the first bins at $q < 0.3$. Therefore, the previously adopted detection threshold seems to be a reasonable choice. Despite the remaining uncertainties, it is clear that $f(q)$ is nearly uniform and does not rise dramatically at $q < 0.3$.

An interesting conclusion from this study is that the PSC companions within $30''$ from the targets with $J_{\text{abs}} < 7$ and suitable $J - K$ colors are physical with a probability of $\geq 84\%$. Many of those companions not listed in the WDS are strong candidates for checking their status with second-epoch imagery. This will lead to the census of visual companions around N_{sample} G-dwarfs complete down to $q \sim 0.2$.

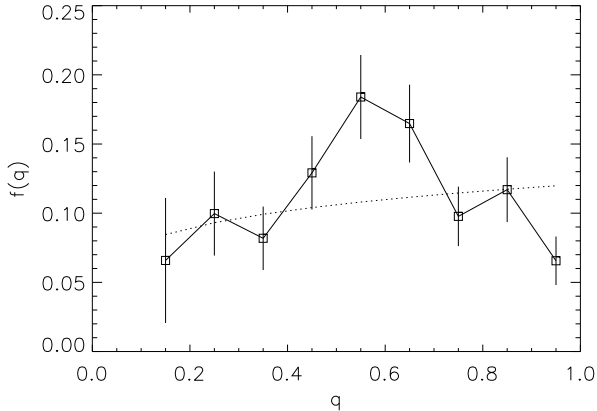


Fig. 15.— Histogram of mass ratio for PSC companions between $10''$ and $30''$ corrected for contamination. The dotted line is a power-law fit with $\beta = 0.19$.

6. Discussion

The sample of low-mass visual companions assembled in Section 4 can still be biased. On one hand, some known pairs with large q are excluded because they do not appear in the PSC. On the other hand, some low-mass companions are missed because their physical status could not yet be confirmed. The total number of missed companions in each of these two groups is $\sim 10\%$ of the total number of binaries. Their inclusion would slightly increase the estimated companion fraction ϵ and would affect $f(q)$, although not dramatically. The largest uncertainty of the derived $f(q)$ is related to the adopted model of the companion detection limit in the PSC.

I intentionally ignored inner sub-systems. The masses are estimated from the total light in the K band. For unresolved sub-systems, these estimates are closer to the mass of their primary components than to the total mass. As the knowledge of sub-systems is currently very incomplete (especially for the secondary companions), correction for them could be only partial. The $f(q)$ derived here remains a preliminary estimate until the multiplicity survey of the sample is done to enable a reasonably comprehensive account of the inner sub-systems.

The distribution of the mass ratio q of wide companions to solar-type dwarfs is found here to be nearly uniform. These binaries have typical

projected separations of 10^3 AU and orbital periods on the order of 10^7 days. Metchev & Hillenbrandt (2009) find a similar mass-ratio distribution with $\beta = -0.39 \pm 0.36$ in a sample of 30 closer companions to solar-type stars surveyed with adaptive optics. A mass-ratio distribution with $\beta \sim -0.5$ was derived by Shatsky & Tokovinin (2002) for visual companions to B-type stars in the Sco OB2 association, while Kraus et al. (2008) found a nearly flat $f(q)$ for low-mass visual binaries in this association. Anyway, the conclusion of Duquennoy & Mayor (1991) that masses of wide companions to G-dwarfs match random selection from the initial mass function is now firmly refuted.

Possible dependence of $f(q)$ on the orbital period remains a debatable subject. Duquennoy & Mayor (1991) found no convincing evidences of any such dependence in their 22-pc sample of 164 G-dwarfs. However, modern study by Raghavan et al. (2010) of the 25-pc sample containing 454 dwarf stars does show a clear trend to smaller q in wide binaries, while short-period pairs prefer equal-mass components (cf. their Fig. 17). They find that the mass-ratio distribution integrated over all periods is remarkably flat and declines at $q < 0.1$. It seems well established that for spectroscopic binaries with orbital periods below 10^3 d the $f(q)$ is nearly flat (Mazeh et al. 2003; Halbwachs et al. 2003). The mass-ratio distribution in the inner sub-systems of multiple stars with solar-type primaries also appears to be flat, to the best of our knowledge (Tokovinin, Hartung, & Hayward 2010).

The frequency of companions to solar-type stars with orbital periods on the order of 10^7 d is around 0.08 per decade of period, or 0.12 per decade of separation according to both Duquennoy & Mayor (1991) and Raghavan et al. (2010). The companion frequency estimate obtained here, 0.13 ± 0.015 , is essentially the same, but more accurate statistically, owing to the larger number of binaries.

This work shows the great potential of the 2MASS PSC for discovering new low-mass companions. Further observations are needed to confirm candidate companions at larger separations and in other, yet un-surveyed, parts of the sky in order to reach complete census of wide binaries in N_{sample} . Combination of this information with spectroscopic and adaptive-optics surveys of the

same sample will open a unique possibility to obtain comprehensive statistics of binary and multiple systems with unprecedented accuracy and detail. This, in turn, will advance our understanding of star formation and our origins.

I thank SMARTS observers J. Vasquez, A. Miranda, and J. Espinosa for making observations and SMARTS data archive at Yale managed by S. W. Tourtellotte for pre-processing and delivering the images. The help of J. Subasavage with astrometric calibration is much appreciated. This work used the 2MASS data products, WDS catalog, ADS services, and SIMBAD.

Facilities: SMARTS

REFERENCES

- Bate, M. R. 2008, MNRAS, 392, 590
- Chauvin, G., Lagrange, A.-M., Bonavita, M., Zuckerman, B., Dumas, C., Bessell, M. S., Beuzit, J.-L., Bonnefoy, M., Desidera, S., Farahi, J., Lowrance, P., Mouillet, D., & Song, I. 2010, A&A, 509, A52
- Cutri, R. M., Skrutskie, M. F., van Dyk, S., Beichman, C. A., Carpenter, J. M., Chester, T., Cambresy, L., Evans, T., Fowler, J., Gizis, J. et al. 2003, The IRSA 2MASS All-Sky Point Source Catalog. NASA/IPAC Infrared Science Archive.
- DePoy, D. L., Atwood, B., Belville, S. R., Brewer, D. F., Byard, P. L., Gould, A., Mason, J. A., O'Brien, T. et al. 2003, Proc. SPIE, 4841, 827
- Duquennoy, A. & Mayor, M. 1991, A&A, 248, 485
- ESA 1997, The Hipparcos and Tycho Catalogues, ESA SP-1200
- Halbwachs, J. L., Mayor, M., Udry, S., & Arenou, F. 2003, A&A, 397, 159
- Henry, T. J. & McCarthy, D. W. 1993, AJ, 106, 773
- Kirkpatrick, J. D., Looper, D. L., Burgasser, A. J. et al. 2010, arXiv:1008.3591
- Koen, C., Kilkeny, D., van Wyk, F., & Marang, F. 2010, MNRAS, 403, 1949
- Kraus, A. L., Ireland, M. J., Martinache, F., & Lloyd, J. P. 2008, ApJ, 679, 762
- Lang, K. R. 1992, Astrophysical data. Planets and Stars (Berlin: Springer-Verlag)
- Lépine, S. & Bongiorno, B. 2007, AJ, 133, 89
- Makarov, V.V. & Kaplan, G.H. 2005, AJ, 129, 2420
- Makarov, V. V., Zacharias, N., & Hennessy, G. S. 2008, ApJ, 687, 566
- Mason, B. D., Wycoff, G. L., Hartkopf, W. I., Douglass, G. G. & Worley, C. E. 2001, AJ 122, 3466 (see the current version at <http://www.usno.navy.mil/USNO/astrometry/optical-IR-pro>)
- Mazeh, T., Simon, M., Prato, L., Markus, B., & Zucker, S. 2003, ApJ, 599, 1344
- Metchev, S. A. & Hillenbrandt, L. A. 2009, ApJS, 181, 62
- Mugrauer, M. & Neuhäuser, R. 2009, A&A, 494, 373
- Nordström, B., Mayor, M., Andersen, J., Holmberg, J., Pont, F., Jorgensen, B. R., Olsen, E. H., Udry, S. & Mowlavi, N. 2004, A&A, 418, 989
- Poveda, A. & Allen, C. 2004, Rev. Mex. Astron. Astrofis., 21, 49
- Press, W. H., Teukolsky, S. A., Vetterling, W. T., & Flannery, B. P. Numerical Recipes in C. Cambridge Univ. Press, Cambridge, UK.
- Raghavan, D., McAlister, H. A., Henry, T. J., Latham, D. W., Marcy, G. W., Mason, B. D., Gies, D. R., White, R. J., & ten Brummelaar, Th. A. 2010, ApJS, 190, 1
- Shatsky, N. & Tokovinin, A. 2002, A&A, 383, 92
- Tokovinin, A., Hartung, M., & Hayward, Th. L. 2010, AJ, 140, 510
- van Leeuwen, F. 2007, A&A, 474, 653
- Vogt et al. 2002, ApJ, 568, 352
- Zacharias, N., Monet, D.,G., Levine, S.,E., Urban, S.,E., Gaume, R., & Wycoff, G. L. 2004a, AAS, 205, 4815

Zacharias, N., Urban, S. E., Zacharias, M. I.,
Wycoff, G. L., Hall, D. M., Monet, D. G., &
Rafferty, T. J. 2004b, AJ, 127, 3043

TABLE 1
COMPANION MEASUREMENTS (2010.14)

HIP	Sys	2MASS				ANDICAM (K)				ANDICAM (V)			
		ρ''	θ_{\circ}	ΔK mag	Q	ρ''	θ_{\circ}	ΔK mag	S	ρ''	θ_{\circ}	ΔV mag	S
9499	AB	12.20	225.2	6.83	A	12.59	224.9	6.77		12.63	225.7	7.48	
10621	AB	18.84	202.6	5.93	A	18.39	202.2	6.09		18.43	203.0	7.64	
11024	AB	10.29	81.1	1.24	A	10.34	82.2	1.21		10.05	79.6	2.52	
11417	AB	19.41	297.7	3.85	A	19.82	297.6	3.80		19.48	297.2	6.81	
11537	AB	3.70	346.5	0.39	D	4.14	343.3	3.15		4.15	345.2	5.36	
11909	AB	15.76	116.9	6.11	A	15.83	117.1	6.17	S				
12764	AB	5.12	271.6	1.83	D	5.77	273.4	3.85					
13544	AB	18.45	23.8	0.10	A	18.05	22.3	0.35		18.29	23.6	0.83	
14774	AB	15.98	245.7	5.83	A	16.00	246.7	5.83					
15247	AB	12.75	293.6	6.55	A	14.19	293.5	6.73					
16540	AB	9.16	32.7	3.19	A	9.16	31.6	3.10		8.99	30.6	6.15	
16853	AB	18.30	261.9	3.70	A	18.96	263.6	3.67		19.10	262.6	4.69	
17936	AB	5.09	304.0	1.78	A	4.93	302.8	3.38		5.03	302.4	5.42	
18261	AB	15.28	263.8	2.99	A	15.44	264.8	3.03		15.51	264.9	5.96	
18305	AB	17.43	304.0	4.24	A	17.94	294.7	4.23		17.50	294.6	5.09	
18713	AB	19.93	287.7	6.44	A	21.99	288.4	6.50		21.56	287.5	7.35	
20366	AB	17.49	13.7	5.50	A	17.19	13.3	5.87		17.61	14.0	6.64	
21220	AB	18.72	358.8	4.95	A	18.62	357.4	4.92		18.24	358.6	7.47	S
21960	AB	19.70	266.0	3.99	A	19.98	267.5	3.92	S	19.66	266.8	7.06	S
22538	AB	7.00	268.2	1.99	A	7.25	272.0	1.98		7.09	271.4	5.47	
22550	AB	14.89	184.9	4.59	A	14.66	187.2	4.52		14.71	189.5	6.58	S
22717	AB	16.51	300.1	5.97	A	16.85	298.9	6.07	S	15.89	304.3	8.42	S
23042	AB	13.76	221.8	6.35	A	11.52	235.9	6.95		11.61	238.4	7.47	S
23742	AB	9.72	358.5	3.83	A	9.77	356.9	3.74		9.96	358.2	6.43	
24221	AB	14.51	140.5	8.06	A	14.59	142.0	7.38	S				
24774	AB	16.46	113.9	-1.10	A	16.41	114.8	-0.65	S	15.94	114.4	1.37	
25148	AB	14.60	226.4	2.53	A	14.43	226.6	1.75	S	14.42	227.9	4.66	
25662	AB	5.54	71.0	1.74	B	5.70	71.0	1.07	S	5.76	67.2	4.50	S
25662	AC	8.54	3.1	4.26	A	11.31	357.0	3.08	S	11.14	358.9	7.25	S
25662	AD	16.85	245.1	2.76	A	16.81	254.7	1.52	S	16.93	254.2	6.19	S
25670	AB	6.58	191.7	2.83	E	6.27	192.3	2.71		6.34	195.2	5.56	
25905	AB	17.15	158.4	6.35	A	11.92	157.7	6.39		11.48	159.9	7.00	
26027	AB	15.52	355.7	5.52	A	15.31	353.3	5.58					
26030	AB	14.96	124.3	6.62	A	15.24	130.7	6.40					
26604	AB	6.17	318.3	0.35	A	6.36	316.4	0.39		6.48	316.6	0.66	
26604	AC	19.78	100.0	5.40	A	19.98	99.2	5.42		19.56	98.6	6.17	
26977	AB	4.35	83.3	1.06	D	4.85	78.2	3.25		4.74	78.2	5.92	
27185	AB	9.36	0.0	3.06	A	9.56	357.4	3.02		9.36	359.6	6.09	S
27957	AB	19.46	262.9	6.09	A	19.76	260.7	5.96		19.42	260.4	8.08	
28419	AB	14.47	75.6	3.88	A	14.15	76.7	3.89		14.05	75.7	7.34	
28604	AB	19.27	46.9	4.11	A	17.70	56.4	4.20		17.75	55.5	5.76	
28671	AB	6.89	226.8	2.24	A	6.74	229.9	2.20		6.54	230.8	3.74	
28671	AC	15.66	163.9	3.59	A	8.25	202.8	3.51		8.36	202.7	4.52	
29444	AB	16.33	16.4	4.50	A	14.47	16.1	4.43		14.61	15.6	7.52	
29673	AB	12.00	308.2	5.15	A	11.85	306.2	5.17	S	11.81	306.3	6.24	S
30114	AB	19.70	84.2	4.72	A	18.65	84.3	4.97		18.60	83.2	4.82	S
31201	AB	18.57	212.5	7.78	A	19.70	214.3	8.00	S	19.65	214.1	9.07	S
31207	AB	9.28	120.8	6.17	U	9.01	117.5	8.04					
31435	AB	11.23	359.8	5.39	A	13.14	355.1	5.72		13.13	355.7	7.20	
31692	AB	15.07	105.7	5.53	A	18.10	114.9	5.64		17.61	114.6	6.90	
33301	AB	9.49	348.2	3.37	A	9.86	346.2	3.34		9.74	347.8	6.41	
33301	AC	16.65	357.6	6.54	E	53.06	247.2	4.34		53.30	246.9	5.78	
34212	AB	11.41	238.2	5.31	A	11.40	239.9	5.27		10.98	241.2	7.94	
34961	AB	15.39	304.3	5.84	A	13.39	296.5	6.05		12.94	297.4	6.77	
35374	AB	19.35	37.4	3.91	A	19.10	36.3	3.78		19.44	36.6	3.42	
36071	AB	6.62	140.1	3.12	A	6.58	137.7	3.39		5.96	137.5	6.32	S
36414	AB	11.74	147.8	4.44	A	12.66	147.4	4.38		12.17	148.7	6.30	S

TABLE 1—*Continued*

HIP	Sys	2MASS				ANDICAM (K)				ANDICAM (V)			
		ρ	θ	ΔK mag	Q	ρ	θ	ΔK mag	S	ρ	θ	ΔV mag	S
36832	AB	7.77	52.6	3.96	A	7.70	49.9	4.10	S	7.61	49.5	7.37	S
37718	AB	15.48	191.1	6.86	U	16.17	185.7	7.99	S				
39999	AB	6.63	33.9	3.42	A	6.83	33.1	4.01		6.66	31.7	6.66	
40765	AB	19.50	113.0	4.03	A	19.88	114.5	4.01		19.34	114.1	6.44	
41620	AB	19.91	241.7	3.93	A	19.37	242.4	3.59	S	19.71	241.7	4.59	S
41871	AB	18.94	50.7	4.61	A	18.75	50.8	4.58		18.62	51.1	8.21	
42344	AB	13.07	74.0	4.57	A	12.74	74.5	4.58		12.74	72.6	7.66	S
44579	AB	18.34	120.3	4.53	A	18.30	119.2	4.30	S	17.70	119.7	4.50	S
44777	AB	12.70	261.5	3.40	A	12.88	261.9	2.86	S	12.95	262.4	5.85	S
44804	AC	6.50	270.6	0.43	A	7.71	277.7	0.42		7.64	277.1	1.26	
44804	AB	7.18	135.4	1.14	A	7.13	134.9	1.10		6.67	135.3	1.82	
44851	AB	11.25	156.7	3.36	A	11.05	155.7	3.28		10.96	156.8	6.83	
47312	AB	4.60	241.0	1.30	D	5.31	243.3	3.49	S				
47947	AB	12.00	228.7	3.10	A	11.74	229.1	3.06		11.64	229.2	5.85	
48146	AB	18.56	277.1	2.39	A	18.86	279.3	2.48		18.71	278.5	2.46	
49285	AB	14.71	252.6	4.67	A	12.09	249.4	4.67		12.21	247.8	5.28	
49913	AB	18.41	233.8	1.26	A	16.70	227.1	1.30		16.82	226.3	2.90	
50100	AB	8.58	169.0	3.44	A	8.41	166.4	3.53		8.29	170.1	6.85	S
51074	AB	17.23	206.1	2.59	A	16.86	205.8	2.51		17.02	206.6	5.38	
52145	AB	6.11	106.4	3.58	A	6.15	106.8	4.06		5.28	107.9	6.03	S
52559	AB	6.12	209.4	1.84	A	6.10	211.7	1.77		6.02	214.3	4.29	
52676	AB	10.32	288.9	3.20	A	10.50	289.5	2.53	S	10.13	289.4	4.79	S
53306	AB	13.68	126.7	3.98	A	13.55	125.5	3.98		13.44	127.0	7.07	
54366	AB	11.92	236.4	4.01	A	11.68	238.4	3.99		11.73	239.5	6.91	
54887	AB	8.14	99.7	2.73	A	8.12	100.0	2.75		7.45	97.7	5.06	
55666	AB	18.95	193.4	5.62	A	17.51	190.5	5.61		17.38	193.1	6.87	
56282	AB	15.85	255.4	4.34	A	15.96	257.7	4.27		15.73	257.4	7.55	
56441	AB	11.81	353.8	2.72	E	11.84	351.0	2.71		11.92	352.0	5.34	
57587	AB	18.59	163.8	5.46	A	18.04	162.6	5.22	S	17.85	164.2	8.24	S
58180	AB	13.39	156.9	2.71	A	13.06	155.4	2.65		12.87	157.5	5.81	
58240	AB	18.85	81.9	0.11	A	18.54	82.1	0.02		18.32	81.3	0.13	
58582	AB	14.29	269.4	5.45	A	12.90	271.4	5.45		12.70	271.6	6.08	
61698	AB	15.88	4.0	4.18	A	15.84	4.6	4.19		15.72	6.2	4.05	
61698	AC	16.79	175.5	2.44	A	16.68	171.8	2.33		16.63	173.2	4.39	
61698	AD	19.25	19.2	4.30	A	19.00	19.8	4.36		19.13	20.4	5.77	
62860	AB	10.68	320.8	5.15	A	11.09	319.9	5.13		11.06	321.2	5.38	S
62925	AB	14.74	147.9	4.14	A	14.94	146.3	4.13		14.42	147.1	7.29	S
63559	AB	17.56	152.6	6.76	A	19.32	133.3	6.92		18.74	134.5	7.54	
64459	AB	8.05	333.4	4.38	A	8.48	330.6	4.67	S	8.10	331.6	6.76	S
65356	AB	12.12	289.4	5.67	A	12.46	289.4	5.64		12.10	290.2	5.99	S
67121	AB	14.85	239.4	1.95	A	13.36	237.8	1.98		13.47	238.7	2.92	
68038	AB	8.68	203.6	4.15	A	8.47	204.6	4.36					
68507	AB	6.68	64.1	3.54	A	6.83	62.8	4.00		6.31	65.4	6.88	S
68507	AC	14.05	245.2	4.86	A	13.36	247.9	4.76		13.19	247.2	5.73	S
68805	AB	3.75	355.7	0.56	C	4.34	347.6	3.49					
69281	AB	12.61	274.3	5.62	A	12.68	274.6	5.57					
69964	AB	14.87	206.1	6.45	A	14.49	202.8	6.51					
70181	AB	3.74	349.2	0.44	A	4.37	347.9	2.34		4.31	347.0	4.78	
70181	AC	19.04	336.8	4.99	A	17.47	340.2	4.99		17.13	341.5	7.07	S
70330	AB	16.00	264.2	4.23	A	13.32	275.4	4.18		13.23	275.3	4.30	
71682	AB	18.88	133.2	4.79	A	18.47	131.9	4.73		17.83	132.5	5.40	S
72998	AB	18.16	51.5	5.48	A	21.82	47.1	5.77		22.23	46.9	5.61	
73815	AB	10.23	315.9	4.76	A	11.60	325.3	5.23		11.49	327.9	5.25	
74888	AB	18.21	107.7	5.06	A	18.16	108.2	4.97		17.82	107.1	6.63	S
76572	AB	14.21	314.4	2.09	A	14.37	315.1	2.12		14.07	315.4	2.39	
77203	AB	19.30	112.7	5.19	A	19.88	111.7	5.24		19.28	111.6	6.36	S
78136	AB	7.88	276.8	4.52	E	8.07	278.2	4.48					

TABLE 1—*Continued*

HIP	Sys	2MASS				ANDICAM (K)				ANDICAM (V)			
		ρ ''	θ °	ΔK mag	Q	ρ ''	θ °	ΔK mag	S	ρ ''	θ °	ΔV mag	S
79048	AB	10.35	356.4	4.57	E	7.55	18.3	7.34	S	7.66	21.0	7.35	S
79143	AB	14.06	153.0	4.16	A	12.03	136.1	4.09	S	11.65	135.6	3.73	S
79169	AB	9.38	265.6	3.24	A	9.48	265.7	3.21		9.39	267.3	6.09	
80784	AB	10.61	304.3	4.59	A	12.97	310.7	4.61		12.67	311.4	6.52	
81274	AB	16.60	275.6	3.35	A	16.94	276.3	3.35		16.69	275.1	6.60	
82384	AB	19.08	208.7	3.96	A	18.70	208.5	3.92		18.96	209.3	7.05	
83083	AB	18.70	51.7	7.89	A	17.72	57.3	8.17	S				
84866	AB	10.14	107.3	3.65	A	10.12	107.6	3.65		9.91	107.1	6.43	
85141	AB	19.26	296.8	6.14	A	19.48	297.0	6.36		18.70	297.0	8.08	
85307	AB	5.36	297.6	2.77	C	6.33	300.2	4.53	S	5.80	300.9	6.16	S

TABLE 2
PHOTOMETRY AND COMPANION STATUS

HIP	π_{HIP} mas	Primary target					Companion								
		N^*	V	J	K_S	M_1 M_{\odot}	ρ''	θ_{\circ}	V	J	K_S	M_2 M_{\odot}	WA	O	
9499	15.3	11	8.07	6.94	6.58	1.15	B	12.20	225	15.55	14.05	13.41	0.10	01	-2.0
10175	24.4	13	8.66	6.91	6.58	0.90	B	6.04	243	9.13	7.21	6.85	0.84	10	2.0
10305	25.2	14	5.65	5.05	4.33	1.52	B	16.79	233	6.69	6.54	6.17	0.97	10	2.0
10579	17.2	6	9.24	8.31	7.97	0.77	B	6.70	288	9.66	8.65	8.24	0.72	10	2.0
10621	16.9	13	7.78	6.85	6.56	1.09	B	18.84	202	15.42	13.08	12.49	0.13	01	-1.0
10710	15.9	13	8.93	7.72	7.33	0.94	B	14.39	312	-	10.79	9.94	0.50	00	0.0
11024	24.4	10	7.87	6.72	6.36	0.95	B	10.29	81	10.39	8.31	7.61	0.70	11	2.0
11324	19.0	6	9.26	8.15	7.88	0.75	B	15.33	165	9.37	8.39	8.12	0.71	10	2.0
11417	17.9	7	8.43	7.10	6.66	1.04	B	19.41	297	15.24	11.35	10.51	0.31	01	2.0
11537	16.7	8	9.25	7.71	7.15	0.95	B	3.70	346	14.61	8.07	7.54	0.87	01	1.0
11586	18.7	8	7.13	6.19	5.89	1.22	B	10.18	305	15.00	10.56	9.82	0.43	10	2.0
11866	19.5	16	7.88	6.79	6.42	1.05	B	7.04	107	13.00	9.43	8.62	0.62	10	1.0
11909	16.6	16	6.84	5.86	5.53	1.41	B	15.76	116	-	12.41	11.64	0.18	01	2.0
12048	25.7	7	6.82	5.68	5.27	1.20	B	5.70	187	-	9.27	8.77	0.52	10	1.0
12764	23.8	15	7.07	6.12	5.80	1.10	B	5.12	271	-	8.60	7.63	0.71	01	1.0
12780	24.2	9	6.95	5.82	5.47	1.18	B	12.48	192	8.50	7.57	7.01	0.81	10	2.0
13027	29.8	15	7.32	5.87	5.52	1.04	B	3.07	308	8.11	5.97	5.64	1.02	10	2.0
13269	17.1	18	6.63	5.55	6.69	1.05	B	17.19	14	-	13.55	12.33	0.13	00	0.0
13544	19.0	10	10.71	8.55	8.26	0.68	B	18.45	23	11.54	8.78	8.36	0.67	11	1.0
14194	18.8	11	7.51	6.60	6.33	1.09	B	8.69	222	9.85	7.87	7.31	0.86	10	2.0
14774	15.3	6	8.06	7.09	6.80	1.09	B	15.98	245	-	13.62	12.62	0.13	01	1.0
15247	20.3	10	7.49	6.46	6.10	1.11	B	12.75	293	16.65	13.56	12.65	0.10	01	-1.0
15868	20.3	9	7.52	6.39	6.05	1.13	B	16.96	253	13.50	9.73	8.86	0.57	10	2.0
16021	15.9	8	8.65	7.64	7.38	0.93	B	15.54	257	11.27	9.52	8.86	0.65	10	2.0
16540	19.8	19	7.49	6.53	6.25	1.08	B	9.16	32	13.64	10.21	9.44	0.50	01	1.0
16794	17.2	9	8.63	7.34	6.94	0.99	B	15.70	358	11.90	9.59	8.78	0.63	10	2.0
16853	23.1	10	7.63	6.49	6.14	1.03	B	18.30	261	12.32	10.47	9.83	0.33	11	-2.0
17936	30.3	15	7.72	6.48	6.15	0.89	B	5.09	303	13.14	8.08	7.93	0.58	01	1.0
18261	21.6	8	7.97	6.86	6.49	0.98	B	15.28	263	7.69	10.32	9.48	0.44	01	2.0
18305	17.2	13	7.70	6.79	6.54	1.09	B	17.43	304	12.79	11.36	10.78	0.28	01	-2.0
18402	17.5	14	7.58	6.53	6.18	1.18	B	2.96	81	11.33	6.72	6.44	1.11	10	1.0
18713	15.2	7	9.11	7.87	7.49	0.92	B	19.93	287	16.46	14.59	13.94	0.08	01	-2.0
18714	20.6	14	8.39	7.20	6.88	0.91	B	8.67	159	14.70	9.60	8.73	0.58	10	2.0
20366	15.4	17	8.71	7.49	7.15	0.99	B	17.49	13	15.35	13.42	12.65	0.13	01	-1.0
20552	36.1	14	6.81	5.68	5.32	0.99	B	5.52	246	7.23	5.89	5.55	0.94	10	2.0
20606	18.3	7	7.71	6.39	6.01	1.20	B	4.30	262	13.80	7.60	6.82	0.99	10	1.0
20769	15.4	15	7.87	6.88	6.62	1.13	B	6.81	182	9.71	8.19	7.77	0.86	10	2.0
20998	19.4	24	7.67	6.48	6.11	1.13	B	17.83	347	-	13.44	10.52	0.28	00	-1.0
21220	16.3	19	8.09	7.11	6.87	1.03	B	18.72	358	15.56	12.72	11.81	0.17	01	-0.5
21960	36.6	15	7.61	6.25	5.80	0.88	B	19.70	266	14.67	10.58	9.79	0.19	01	2.0
21963	18.2	18	8.04	6.97	6.62	1.04	B	8.14	92	13.30	9.59	8.75	0.62	10	2.0
22538	15.3	16	8.58	7.62	7.32	0.96	B	7.00	268	14.05	10.01	9.30	0.59	01	1.0
22550	21.3	34	6.75	5.71	5.44	1.27	B	14.89	184	13.33	10.71	10.03	0.33	11	-1.0
22717	30.8	52	6.29	5.33	4.98	1.17	B	16.51	300	14.71	11.47	10.96	0.14	01	-1.0
23042	16.9	22	8.94	7.71	7.32	0.91	B	13.76	221	16.41	14.47	13.68	0.08	01	-1.0
23742	17.9	21	7.73	6.72	6.41	1.10	B	9.72	358	14.16	10.71	10.24	0.36	01	1.0
23926	18.7	14	6.75	5.51	5.10	1.47	B	10.11	260	10.29	8.47	7.90	0.75	10	2.0
24221	16.3	50	7.04	6.20	5.92	1.30	B	14.51	140	16.01	14.81	13.98	0.07	01	-1.0
24320	17.4	21	8.82	7.61	7.14	0.94	B	4.67	141	9.90	8.00	7.58	0.84	10	2.0
24711	15.3	19	8.37	7.31	6.95	1.05	B	13.32	170	10.57	8.81	8.24	0.77	10	2.0
24774	18.6	30	9.20	8.32	7.99	0.74	B	16.46	113	10.57	7.89	6.89	0.96	11	-2.0
25082	17.6	29	7.00	6.12	5.85	1.27	B	9.51	39	10.43	8.62	8.09	0.74	10	2.0
25148	15.1	21	8.75	7.45	6.97	1.05	B	14.60	226	13.41	10.32	9.51	0.57	01	2.0
25662	35.5	45	6.74	5.61	5.33	1.00	B	5.54	71	11.24	7.59	7.07	0.66	01	2.0
							C	8.54	3	13.99	10.35	9.59	0.22	01	-1.0
							D	16.85	245	12.93	9.18	8.09	0.51	01	-1.0
25670	20.6	20	8.27	7.08	6.73	0.95	B	6.58	191	13.83	9.88	9.56	0.45	01	2.0

TABLE 2—Continued

HIP	π_{HIP} mas	Primary target					M_1 M_{\odot}	Companion							
		N^*	V	J	K_S	ρ''		θ_{\circ}	V	J	K_S	M_2 M_{\odot}	WA	O	
25905	25.7	37	8.38	7.06	6.66	0.86	B	17.15	158	15.38	13.71	13.00	0.07	01	-2.0
26027	16.4	70	8.20	7.18	6.88	1.03	B	15.52	355	17.05	13.21	12.40	0.13	01	1.0
26030	15.9	57	8.60	7.48	7.11	0.99	B	14.96	124	-	14.65	13.73	0.08	01	-2.0
26060	19.8	19	7.73	6.69	6.38	1.05	B	3.79	22	11.24	7.15	6.90	0.93	10	-1.0
26404	17.5	18	8.07	6.80	6.50	1.09	B	3.54	259	13.20	7.84	6.79	1.01	10	-1.0
26604	16.2	56	8.73	7.62	7.21	0.96	B	6.17	318	9.39	8.03	7.56	0.88	11	2.0
							C	19.78	99	14.90	13.15	12.61	0.12	01	-1.0
26977	19.4	23	8.71	7.43	7.00	0.92	B	4.35	83	14.63	8.28	8.06	0.71	01	-2.0
27185	16.0	20	8.10	7.14	6.78	1.07	B	9.36	0	14.19	10.55	9.84	0.51	01	1.0
27922	42.4	24	7.51	6.21	5.76	0.82	B	10.62	19	10.65	7.99	7.22	0.58	10	2.0
27957	16.8	35	8.39	7.25	6.90	1.01	B	19.46	262	16.47	13.89	12.99	0.10	01	-2.0
28241	16.0	22	8.26	7.15	6.81	1.06	B	11.03	46	-	10.65	9.84	0.51	10	1.0
28403	19.6	27	8.61	7.40	7.05	0.90	B	15.76	216	12.50	13.68	12.86	0.10	10	-2.0
28419	15.5	25	8.60	7.47	7.10	1.00	B	14.47	75	15.94	11.81	10.98	0.28	01	1.0
28604	19.5	22	8.73	7.55	7.18	0.87	B	19.27	46	14.49	12.07	11.29	0.18	01	-2.0
28671	16.8	84	9.31	8.00	7.58	0.86	B	6.89	226	13.83	10.59	9.82	0.50	11	2.0
							C	15.66	163	13.05	11.73	11.18	0.23	01	-2.0
28790	37.2	18	5.96	5.08	4.75	1.12	B	5.67	215	9.16	6.60	6.03	0.82	10	2.0
29444	19.4	41	8.16	7.19	6.90	0.94	B	16.33	16	15.68	12.52	11.41	0.17	01	-2.0
29673	31.8	64	6.62	5.57	5.21	1.09	B	12.00	308	12.86	10.89	10.36	0.17	01	-2.0
30114	19.8	74	7.70	6.51	6.11	1.12	B	19.70	84	12.52	11.06	10.84	0.22	01	-2.0
30158	17.8	21	8.47	7.29	6.91	0.98	B	7.04	7	10.76	8.63	8.03	0.75	10	2.0
31201	16.2	35	6.89	5.89	5.54	1.43	B	18.57	212	15.96	14.03	13.31	0.09	01	-2.0
31207	16.6	32	8.11	7.09	6.79	1.04	B	9.28	120	16.23	14.65	12.96	0.11	01	-2.0
31435	16.8	98	8.09	6.79	6.43	1.13	B	11.23	359	15.29	12.35	11.82	0.16	01	-2.0
31692	25.4	31	8.68	7.31	6.86	0.82	B	15.07	105	15.58	13.19	12.39	0.09	01	-2.0
33301	16.1	49	7.88	6.87	6.60	1.11	B	9.49	348	14.29	10.79	9.97	0.48	01	2.0
							C	16.65	357	13.66	13.82	13.14	0.10	01	-2.0
34212	17.5	34	7.68	6.67	6.36	1.13	B	11.41	238	15.87	12.10	11.67	0.17	01	1.0
34961	18.7	36	9.20	7.75	7.26	0.88	B	15.39	304	15.97	13.90	13.10	0.09	01	-2.0
35374	16.7	47	7.94	6.63	6.17	1.21	B	19.35	37	11.36	10.35	10.07	0.43	01	-1.0
35564	31.5	46	5.98	5.28	4.95	1.16	B	9.08	26	6.63	5.52	5.07	1.13	10	2.0
35733	16.5	80	7.00	6.11	5.81	1.33	B	7.41	191	8.01	7.01	6.68	1.07	10	2.0
36071	28.1	74	6.98	5.97	5.67	1.04	B	6.62	140	13.30	9.49	8.79	0.47	01	0.5
36165	31.2	98	7.02	6.13	5.80	0.95	B	17.66	226	8.06	7.00	6.60	0.79	10	2.0
36414	19.0	84	7.74	6.72	6.44	1.06	B	11.74	147	14.04	11.52	10.88	0.23	11	-2.0
36485	22.0	44	7.30	6.42	6.18	1.04	B	7.77	46	9.47	7.91	7.44	0.77	10	2.0
36763	17.0	61	9.12	7.86	7.42	0.89	B	4.03	242	12.22	8.43	7.90	0.79	10	2.0
36832	34.6	60	7.57	6.17	5.66	0.93	B	7.77	52	14.94	10.39	9.62	0.23	01	2.0
37645	19.6	43	7.02	6.02	5.65	1.26	B	9.53	147	10.51	8.61	7.97	0.72	10	2.0
37718	32.4	65	6.64	5.68	5.36	1.04	B	15.48	191	-	13.30	12.22	0.08	01	-2.0
37735	21.8	34	8.82	7.39	6.99	0.86	B	6.09	128	12.23	9.25	8.40	0.61	10	2.0
39409	15.7	52	9.19	7.83	7.44	0.92	B	5.05	330	9.24	7.87	7.43	0.92	10	2.0
39999	17.5	16	7.60	6.61	6.34	1.13	B	6.63	33	14.26	10.08	9.77	0.49	01	2.0
40765	28.2	42	7.44	6.39	6.01	0.96	B	19.50	113	13.88	11.06	10.03	0.23	01	-0.5
41620	16.9	67	8.50	7.30	6.97	0.99	B	19.91	241	13.09	11.55	10.90	0.26	01	-1.0
41871	26.6	39	7.60	6.46	6.07	0.97	B	18.94	50	15.81	11.51	10.68	0.17	01	2.0
42172	39.8	21	5.91	4.95	4.65	1.11	B	10.18	25	7.16	5.88	5.50	0.90	10	2.0
42344	19.4	93	9.40	7.95	7.44	0.82	B	13.07	74	17.62	12.89	12.01	0.13	01	2.0
42951	16.2	34	6.41	5.74	5.44	1.47	B	4.56	263	7.08	6.22	5.95	1.30	10	2.0
44579	15.5	22	8.59	7.52	7.18	0.99	B	18.34	120	13.09	12.11	11.71	0.19	01	-1.0
44777	21.5	17	8.15	7.06	6.70	0.93	B	12.70	261	14.00	10.95	10.11	0.31	01	2.0
44804	15.5	28	8.64	7.52	7.15	0.99	C	6.50	270	9.90	8.20	7.58	0.89	11	-2.0
							B	7.18	135	10.46	8.85	8.29	0.75	11	2.0
44851	20.5	98	8.24	7.04	6.60	0.98	B	11.25	156	15.07	10.78	9.96	0.36	01	1.0
45734	17.6	52	8.32	7.16	6.78	1.02	B	8.99	194	9.47	7.95	7.44	0.87	10	2.0
45940	28.6	78	8.11	6.90	6.43	0.86	B	6.68	70	11.70	8.95	8.07	0.58	10	2.0

TABLE 2—*Continued*

HIP	π_{HIP} mas	Primary target					M_1 M_{\odot}	Companion							
		N^*	V	J	K_S	ρ''		θ_{\circ}	V	J	K_S	M_2 M_{\odot}	WA	O	
47058	21.3	14	7.78	6.62	6.21	1.05	B	8.12	275	10.34	8.44	7.81	0.72	10	2.0
47312	18.2	16	8.16	6.99	6.61	1.04	B	4.60	241	-	8.28	7.91	0.76	01	1.0
47537	18.1	22	7.65	6.64	6.39	1.10	B	3.20	248	9.44	6.84	6.62	1.04	10	2.0
47862	15.8	11	7.11	6.27	6.02	1.29	B	9.59	174	10.94	8.90	8.27	0.75	10	2.0
47947	19.7	74	7.95	6.84	6.52	1.02	B	12.00	228	13.80	10.42	9.62	0.46	01	2.0
48146	16.7	10	9.59	8.55	8.29	0.72	B	18.56	277	12.05	10.97	10.68	0.30	01	-2.0
49285	21.1	27	8.10	6.86	6.47	0.99	B	14.71	252	13.38	11.70	11.14	0.18	01	-2.0
49442	15.6	31	7.56	6.33	5.99	1.31	B	3.88	261	8.28	6.52	6.33	1.20	10	2.0
49520	16.9	16	8.67	7.60	7.24	0.93	B	9.47	327	8.83	7.70	7.30	0.91	10	2.0
49668	26.6	19	7.28	6.10	5.74	1.05	B	3.90	311	11.07	6.90	6.33	0.91	10	2.0
49913	16.1	95	8.51	7.35	7.02	1.00	B	18.41	233	11.41	9.10	8.29	0.74	01	-2.0
50100	19.3	13	7.21	6.32	6.07	1.15	B	8.58	168	14.06	10.20	9.51	0.50	01	2.0
50681	17.3	27	9.14	7.88	7.45	0.87	B	7.70	320	-	10.85	10.00	0.43	10	1.0
50874	18.7	19	6.64	5.70	5.38	1.38	B	4.25	121	10.14	6.78	6.23	1.12	10	1.0
51074	19.5	76	8.59	7.28	6.85	0.95	B	17.23	206	13.97	10.26	9.44	0.51	01	1.0
52145	20.0	22	7.20	6.33	6.08	1.12	B	6.11	106	13.23	9.73	9.66	0.44	01	1.0
52559	15.1	63	9.03	7.80	7.35	0.96	B	6.12	209	13.32	9.76	9.19	0.61	01	2.0
52676	23.7	42	7.50	6.41	6.07	1.03	B	10.32	288	12.29	10.02	9.27	0.45	01	1.0
53306	25.3	41	8.40	7.11	6.70	0.86	B	13.68	126	15.47	11.54	10.68	0.18	01	2.0
54366	19.6	10	7.80	6.71	6.40	1.05	B	11.92	236	14.71	11.11	10.41	0.29	01	1.0
54887	16.0	7	7.88	6.87	6.60	1.11	B	8.14	99	12.94	10.08	9.33	0.58	01	2.0
55288	20.8	10	7.05	6.09	5.82	1.17	B	9.52	254	7.83	6.63	6.22	1.07	10	2.0
55487	21.9	22	8.13	7.00	6.66	0.93	B	10.69	38	13.00	9.77	8.89	0.54	10	1.0
55666	20.1	10	6.95	5.94	5.62	1.25	B	18.95	193	13.82	11.99	11.24	0.18	01	-2.0
56049	17.4	12	7.44	6.44	6.14	1.19	B	4.43	349	14.60	7.54	7.32	0.90	10	2.0
56242	42.9	7	6.27	5.18	4.90	1.00	B	15.50	330	9.05	7.04	6.37	0.70	10	2.0
56280	38.0	24	5.64	6.68	4.35	1.22	B	9.68	209	5.72	6.66	4.50	1.18	10	2.0
56282	16.1	7	8.08	7.05	6.74	1.07	B	15.85	255	15.63	11.84	11.08	0.25	01	1.0
56441	15.5	9	8.42	7.38	7.09	1.01	B	11.81	353	13.76	10.59	9.81	0.52	01	1.0
57587	23.2	17	6.25	5.17	4.85	1.40	B	18.59	163	14.49	10.97	10.31	0.25	01	-0.5
58180	20.6	79	8.60	7.32	6.91	0.91	B	13.39	156	14.41	10.47	9.63	0.43	01	1.0
58240	21.1	34	7.61	6.49	6.13	1.08	B	18.85	81	7.74	6.60	6.24	1.05	11	2.0
58582	15.5	89	8.14	7.15	6.85	1.06	B	14.29	269	14.22	12.77	12.30	0.15	01	-2.0
59021	19.4	31	6.61	5.49	5.10	1.45	B	5.83	318	8.89	7.11	6.55	1.02	10	2.0
59250	15.1	13	7.78	6.78	6.54	1.16	B	17.42	336	-	11.95	11.12	0.27	00	0.5
59272	45.0	23	6.77	5.65	5.27	0.89	B	9.30	89	9.73	7.31	6.53	0.66	10	2.0
							C	10.66	35	8.12	7.68	7.45	0.53	10	-2.0
59707	34.1	12	7.49	6.23	5.83	0.90	B	3.90	107	14.20	7.11	6.66	0.74	10	1.0
60155	16.5	17	8.34	7.26	6.94	1.01	B	14.74	299	10.69	9.81	9.45	0.55	10	-2.0
60251	17.6	92	9.06	8.00	7.63	0.83	B	14.08	86	12.00	10.00	9.39	0.54	10	-2.0
60337	15.7	7	7.99	7.07	6.78	1.08	B	12.78	38	13.50	11.48	10.86	0.30	10	-2.0
61298	17.5	12	8.80	7.59	7.16	0.93	B	18.74	224	-	10.09	9.23	0.56	00	0.5
61595	17.8	29	8.19	7.06	6.68	1.04	B	8.28	180	10.77	8.79	8.12	0.73	10	2.0
61608	16.1	11	8.81	7.55	7.15	0.97	B	5.52	283	-	9.76	9.33	0.57	00	0.5
61698	17.4	96	8.35	7.26	6.93	0.99	B	15.88	3	12.40	11.37	11.10	0.23	01	-1.0
							C	16.79	175	12.74	10.19	9.37	0.55	01	0.1
							D	19.25	19	14.12	11.99	11.23	0.21	01	-1.0
62860	16.6	11	7.67	6.73	6.48	1.12	B	10.68	320	15.30	12.42	11.63	0.18	01	1.0
62925	20.1	21	7.71	6.69	6.42	1.03	B	14.74	147	15.00	11.54	10.56	0.26	01	1.0
63559	18.0	26	8.06	6.96	6.58	1.05	B	17.56	152	15.60	14.02	13.34	0.09	01	-2.0
64030	15.4	8	7.51	6.60	6.32	1.22	B	7.02	358	8.09	6.96	6.61	1.13	10	2.0
64459	27.7	21	6.70	5.56	5.14	1.19	B	8.05	333	13.46	10.11	9.52	0.32	11	1.0
64498	18.0	13	7.67	6.64	6.25	1.14	B	9.42	301	10.02	8.43	7.85	0.77	10	2.0
65356	18.3	14	8.16	7.04	6.72	1.01	B	12.12	289	16.47	13.24	12.39	0.12	01	1.0
67067	15.6	9	9.35	8.00	7.59	0.89	B	5.21	163	13.51	9.26	8.82	0.66	10	1.0
67121	16.7	52	8.60	7.34	6.99	0.99	B	14.85	239	11.52	9.62	8.95	0.62	01	-1.0
67408	33.9	45	6.58	5.55	5.22	1.05	B	11.60	358	10.09	7.72	7.02	0.68	10	2.0

TABLE 2—*Continued*

HIP	π_{HIP} mas	Primary target					Companion								
		N^*	V	J	K_S	M_1 M_{\odot}	ρ''	θ $^{\circ}$	V	J	K_S	M_2 M_{\odot}	WA	O	
67412	26.5	13	8.50	7.19	6.76	0.82	B	15.69	20	11.00	9.32	8.44	0.55	10	1.0
68038	17.6	20	6.84	5.94	5.67	1.33	B	6.68	203	12.22	10.41	9.83	0.47	01	-1.0
68507	16.2	31	7.58	6.65	6.35	1.17	B	6.68	64	14.46	10.60	9.89	0.50	01	1.0
							C	14.05	245	13.31	11.70	11.21	0.23	11	-2.0
68805	20.7	13	8.08	7.01	6.67	0.96	B	3.75	355	-	7.46	7.22	0.84	01	0.5
69054	15.9	21	7.95	6.94	6.62	1.11	B	5.90	276	9.05	7.59	7.12	0.99	10	2.0
69281	16.5	11	8.31	7.00	6.59	1.10	B	12.61	274	-	12.87	12.21	0.14	01	1.0
69964	18.2	58	9.33	7.96	7.50	0.84	B	14.87	206	16.34	14.69	13.95	0.07	01	-2.0
70181	20.9	15	8.68	7.32	6.88	0.91	B	3.74	349	13.46	8.29	7.32	0.81	01	0.5
							C	19.04	336	16.87	12.76	11.87	0.13	01	-1.0
70269	25.4	17	6.82	6.46	6.09	0.99	B	5.78	174	6.84	6.41	6.05	1.00	10	2.0
70330	18.7	23	7.73	6.61	6.20	1.13	B	16.00	264	12.03	10.82	10.43	0.30	01	-2.0
70386	27.0	22	7.41	6.38	6.07	0.96	B	9.27	334	7.59	6.55	6.21	0.93	10	2.0
71682	23.4	32	7.00	6.07	5.76	1.12	B	18.88	133	12.40	11.00	10.56	0.21	11	-2.0
72235	24.0	49	8.44	7.19	6.80	0.86	B	9.05	26	10.63	8.41	7.68	0.69	10	2.0
72764	20.6	12	8.41	6.99	6.64	0.96	B	8.37	165	12.50	10.00	9.31	0.51	10	1.0
72998	20.2	17	9.53	8.15	7.68	0.76	B	18.16	51	15.14	13.78	13.16	0.08	01	-2.0
73309	29.6	11	6.09	5.14	4.84	1.24	B	9.62	23	13.20	9.24	8.50	0.51	10	2.0
73372	18.8	52	8.74	7.59	7.20	0.89	B	15.20	232	12.50	9.01	7.98	0.73	10	-1.0
73674	22.7	38	8.38	7.26	6.90	0.86	B	7.43	220	8.40	7.26	6.89	0.86	10	2.0
							C	11.22	11	8.40	13.95	13.07	0.08	00	0.0
73815	17.4	16	8.21	7.00	6.65	1.06	B	10.23	315	13.46	11.81	11.41	0.19	01	-2.0
74016	31.7	15	7.25	5.85	5.49	1.02	B	3.82	212	7.48	5.96	5.51	1.01	10	2.0
74734	23.9	12	7.68	6.53	6.17	1.00	B	5.31	292	11.31	7.82	7.73	0.69	10	2.0
74771	26.6	16	8.05	6.81	6.39	0.90	B	6.07	16	9.69	7.79	7.12	0.75	10	2.0
74888	16.6	17	8.77	7.49	7.02	0.99	B	18.21	107	15.76	12.91	12.08	0.15	01	1.0
74930	20.0	10	7.13	6.18	5.88	1.18	B	13.36	167	8.07	6.98	6.62	0.99	10	2.0
74975	39.4	19	5.05	4.34	4.01	1.30	B	11.44	35	10.11	7.49	6.75	0.67	10	2.0
75363	35.0	43	7.52	6.20	5.72	0.91	B	14.28	223	14.00	9.47	8.69	0.38	10	2.0
75790	17.1	49	6.53	5.55	5.19	1.51	B	9.48	9	9.63	8.24	7.73	0.82	10	2.0
76572	17.9	32	10.02	9.17	8.97	0.59	B	14.21	314	12.41	11.31	11.06	0.22	01	-1.0
76603	37.6	33	6.48	5.51	5.15	1.01	B	11.78	189	6.68	5.63	5.32	0.97	10	2.0
77203	15.1	37	7.65	6.77	6.51	1.17	B	19.30	112	14.01	12.28	11.71	0.19	01	-2.0
78024	27.1	23	6.97	5.99	5.66	1.06	B	5.96	352	8.66	7.04	6.60	0.85	10	2.0
78136	15.4	95	8.04	7.06	6.81	1.08	B	7.88	276	-	11.56	11.33	0.23	01	0.5
78738	39.6	24	7.43	6.20	5.79	0.84	B	11.85	98	8.05	6.59	6.11	0.78	10	2.0
79048	31.6	49	7.03	5.97	5.62	0.99	B	10.35	356	14.38	11.80	10.19	0.18	01	-2.0
79143	38.8	100	7.23	5.99	5.55	0.90	B	14.06	153	10.96	10.04	9.72	0.18	01	-2.0
79169	17.7	40	7.86	6.74	6.39	1.11	B	9.38	265	13.95	10.36	9.63	0.51	01	2.0
79396	19.3	26	8.22	7.11	6.75	0.97	B	3.15	173	12.50	7.18	7.02	0.91	10	1.0
79682	20.0	33	8.75	7.57	7.23	0.85	B	15.05	40	14.40	10.03	9.26	0.52	10	1.0
80784	18.5	46	7.96	6.74	6.36	1.10	B	10.61	304	14.48	11.49	10.95	0.23	01	-2.0
81274	16.4	35	8.22	7.15	6.82	1.04	B	16.60	275	14.82	11.00	10.17	0.42	01	2.0
82384	15.5	55	8.83	7.71	7.41	0.93	B	19.08	208	15.88	12.42	11.38	0.22	01	0.5
82416	19.0	88	9.30	8.01	7.59	0.80	B	9.41	172	11.46	9.39	8.61	0.63	10	2.0
83083	19.5	21	6.90	5.69	5.40	1.34	B	18.70	51	16.05	14.05	13.29	0.08	01	-2.0
84866	15.3	79	8.78	7.47	7.05	1.02	B	10.14	107	15.21	11.56	10.70	0.34	01	2.0
85141	17.0	89	7.84	6.64	6.30	1.16	B	19.26	296	15.92	13.14	12.44	0.13	01	-1.0
85307	16.2	73	6.45	5.57	5.30	1.52	B	5.36	297	12.61	8.01	8.08	0.78	01	0.5
87638	18.5	47	8.17	7.02	6.70	1.01	B	5.96	18	11.69	8.68	7.95	0.75	10	2.0

TABLE 3
NOTES ON INDIVIDUAL TARGETS

HIP	Text
9499	A is SB, no orbit. N04: $\Delta RV=70.7$. The B-companion is optical.
10305	A is SB2, period 94.788d, resolved by speckle (TOK 39). A is evolved. B = HIP 10303 is physical.
10579	AB = HJ 3491 is physical. Also CPM with HIP 10754 at $836''$.
10621	NOMAD: PM(B)=(0,-30), PM(A)=(18,60), AB is optical. BC is a binary at $2''54$, 180.0° , $\Delta K=0.47$, $\Delta V=0.89$. There is a CPM companion HIP 10754 at $836''$.
10710	No data. The PSC companion at $14''4$ is likely physical based on the CMD and $N^*=13$.
11324	B = HIP 11323, physical. Both components are below the MS, the true parallax should be 12.6mas (as for the B-component in Hipparcos).
11417	SB, no orbit (N04). NOMAD: PM(B)=(-12,-68), $V=14.73$. B is physical. PM(A)=(-22,-76). A new triple system.
11537	The V-photometry is affected by small separation, $4''$. B is new physical companion, red in the $V - K$ color, variable? Astrometric binary in HIPPARCOS (Makarov & Kaplan 2005), possibly a new triple? SIMBAD: PMS star and X-ray source 1RXS J022843.6-311332.
12048	The component C at $22''4$ is optical. The B-component is physical, estimated mass $0.29 M_\odot$ (Metchev & Hillenbrandt 2009)
12764	A is SB, no orbit (N04: $\Delta RV=2.5$). Contradictory photometry of B, it is too close in 2MASS ($5''$). NOMAD: PM(B)=(-99,-71) $V=7.79$ (??) Considering the brightness of B and $N^*=15$, it is almost certainly physical. A new triple system.
12780	A is visual binary FIN 379, $0''1$. B = HIP 12779, AB = BSO 1 at $12''5$, physical.
13269	The PSC companion at $17''2$ is likely an artifact (not detected in J and H bands). A is an astrometric binary.
13544	B is a known close binary A 2341 of $1''3$ separation partially resolved in the ANDICAM images in K and V bands.
15247	A is SB without orbit, N04: $\Delta RV=6.6$. The faint companion B is confirmed with ANDICAM, it is optical.
15868	A is the close pair A 2909, $0''1$. The PSC companion at $17''$ is called C in the WDS, it is physical.
17936	The magnitude difference in the PSC $\Delta K=1.8$ is suspect ($5''$ separation), $\Delta K=3.4$ is measured with ANDICAM.
18305	NOMAD: PM(B)=(-89,+19), $V=11.48$ (??). B is optical. PM(A)=(+108,+218).
18402	B is definitely physical, but it is too red in the ($K_{\text{abs}}, V - K$) CMD. Infrared companion? Nothing on B in SIMBAD.
18713	NOMAD: PM(B)=(+44,+43). B is optical. PM(A)=(+162,-39).
20366	Small PM(A)=(-31,-12). NOMAD: PM(B)=(+39,-63), $V=13.95$. B is optical based on its $V - K$ color (blue, below the MS).
20606	Both components A,B are above the MS, young? AB - RST 1273 is physical. B is too red in the ($K_{\text{abs}}, V - K$) CMD, infrared companion? Planetary companion to A = HD 28254 is detected with RV. No relevant references in SIMBAD.
20998	Not observed, but $J - K = 2.92$ for B in the PSC, hence optical.
21960	B is new physical companion at $19.7'''$. A was observed with NACO by Eggenberger et al. 2007A&A...474..273E.
22538	B at $7''$, 268° is physical. The original Hipparcos gives parallax 13.9 mas. A is X-ray source 1RXS J045103.5-273115.
23742	ANDICAM confirms the PSC photometry of B in the K-band. B is well below the MS in the CMDs, but it is certainly physical.
23926	B = HIP 23923. AB = HJ 3728, physical. A is above the MS, evolved (despite sp. type G3V). The pair was observed with NICI in 2010. Both A and B have large PM, PM(A)=(-77,+284). The original Hipparcos parallax of B is 8.5mas, obviously wrong. IRAS source.
24221	B at $14''5$ is optical. A is SB without orbit (N04: $\Delta RV=56.7$).
24711	B = HIP 24712. AB = HJ 3745, physical.
24774	The B-companion could possibly be a semi-resolved binary. It is optical anyway.
25148	A is SB without orbit, N04: $\Delta RV=3.7$ and also an astrometric binary (Makarov & Kaplan 2005)
25662	B at $14''6$ is physical, this is a new triple system. Mini-cluster. The components B, C, D are measured (B is physical, C and D optical). There is also LDS 6186 companion at $99''4$, $V=14.23$. A is SB and astrometric pair (Vogt et al. 2002): P=1427d, M2=0.18 M_\odot . The system is thus a new quadruple.
25905	One more component is seen in the ANDICAM images at $23''$, 9° , $\Delta K=5.0$, also likely optical. A is SB without orbit (N04).
26027	Two companions are seen in the ANDICAM images. C is at $10''4$, 75° , bluer than B, is likely optical while B is physical.
26030	B at $15''$ is optical. A is resolved into a new pair Aa,Ab in ANDICAM K-band: $1''6$, 91° , $\Delta K \sim 2.7$.
26404	AB = B 84 = ADS 4227, $3''$. The pair is optical according to the CMDs (B is too red, above the MS). Small PM(A)=(+13,-14). However, the field is not crowded, $N^*=14$, an optical companion at $3''5$ is unlikely. Is B an infrared companion? No relevant references in SIMBAD.
26604	AB = STF 763 = ADS 4545, $6''4$, physical. The PSC companion C at $19''8$ is optical.
27957	B is optical. Several other components are seen in the ANDICAM field, $N^*=35$.
28241	No V-photometry for B in either WDS or SIMBAD.
28403	BC is a close $4''1$ pair, optical to A.
28604	The B-companion could be a close binary (PSF fit), it is optical to A. NOMAD: PM(B)=(+2,+10), $V=14.30$.
28671	Close triple, Aab=HDS 823 at $0''1$. AB = LDS 6195, $6''9$, physical. The PSC companion C at $15''7$ is optical.
28790	HIP 28764 at $196''$ is a CPM companion to this physical pair AB = HJ 3834.
29444	HIP 29439 at $20''6$ is physical, but the PSC companion B at $16''$, 16° is optical.
30114	NOMAD: PM(B)=(0,-1), $V=12.46$. B is optical. PM(A)=(+73,-18).
31201	The PSC companion at $18''6$ is optical, but the $30''$ pair I 755 is physical.
31692	NOMAD lists 5 components, but none fits the PSC source at $15''$ which is optical anyway.

TABLE 3—Continued

HIP	Text
34212	A is SB without orbit (N04: $\Delta RV = 4.3\text{km/s}$), also astrometric binary in Hipparcos. This is a new triple system with the physical PSC companion B at $11''4$.
35374	Quadruple. AB = RST 244 at $3''17$, both A and B are close visual pairs. The PSC component at $19''$ is optical, there are other stars in the ANDICAM frames as well.
36071	The position measurement in the V-band is of low accuracy. The status of the B-companion remains uncertain.
36165	B = HIP 36160. AB = HJ 3969 at $17''7$, physical. The pair has large PM: PM(A) = $(-291, +102)$.
36414	A is an SB without orbit, N04: $\Delta RV = 1.2^*$. The companion B = RSS 132 at $11''7$ is optical.
36832	A is SB without orbit, N04: $\Delta RV = 6.7$. B at $7''8$ is physical. This is a new triple system. The A-component is a PMS star in SIMBAD, chromospherically active, X-ray source. Both components are on the MS, however.
37718	B is optical. NOMAD: PM(B) = $(+11, -7)$. HIP 37727 at $51''9$ is physical.
39999	The PSC companion B at $6''6$ is physical. There is also a CPM companion at $92''6$ (S. Lépine). A new triple system.
40765	Small PM(A) = $(-1, +42)$. NOMAD: PM(B) = $(+66, -16)$, $V(B) = 12.83$. B can be optical (crowded field, $N^* = 42$).
41620	NOMAD: PM(B) = $(-21, -3)$, $V(B) = 13.21$. B is optical based on the CMDs. PM(A) = $(-41, +14)$.
41871	Astrometric binary in Hipparcos. The PSC companion B at $19''$ is physical, a new triple system.
42172	B = HIP 42173. AB = STF 1245 at $10''2$ is physical.
42344	The ANDICAM position in the V-band is not accurate. NOMAD: PM(B) = $(0, +28)$, $V = 16.70$, but B is definitely physical. PM(A) = $(-147, +95)$.
42951	Very small PM(A) = $(+1, -9)$. B is considered physical based on the CMDs and its brightness.
44579	Small PM(A) = $(+28, -33)$. NOMAD: PM(B) = $(+27, -30)$, $V(B) = 12.99$. B is optical, below the MS!
44777	X-ray source 1RXS J090732.0+000352. The companion B at $12''7$ is physical.
44804	Close triple. The companion C at $6''5$ is optical, while B at $7''2$ is physical. Observed with NICI (Tokovinin, Hartung, & Hayward 2010).
44851	NOMAD: PM(B) = $(+102, +500)$ $V = 16.37$ (?). B is physical, despite crowded field with $N^* = 98$. PM(A) = $(-59, -3)$. PMS star, X-ray source RXS J090817.3-370649, variable CY Pyx.
45734	Aab is a $0''1$ pair KOH83, also observed with NICI. B is SB2 without orbit. This is a PMS quadruple, both components are slightly above the MS.
47312	A is SB without orbit, N04: $\Delta RV = 18.7$. This is a new triple system with the physical PSC companion at $4''6$.
48146	NOMAD: PM(B) = $(+2, -4)$, $V(B) = 12.01$. B is optical. PM(A) = $(+12, -59)$.
49285	NOMAD: PM(B) = $(-19, +2)$, $V = 12.97$. B is optical. PM(A) = $(-236, +29)$.
49913	NOMAD: PM(B) = $(-9, +8)$. B is optical (however, it is on the MS in both CMDs). PM(A) = $(-272, +83)$. Crowded field, $N^* = 95$.
50100	B at $8''6$ is physical. A is X-ray source 1RXS J101344.5-072301.
50681	No V-band photometry in the WDS. AB = RSS 233 is physical.
52145	A is SB without orbit, N04: $\Delta RV = 1.2$. A new triple. There is also a bright companion C in the field.
52676	B at $10''3$ is physical. Planet-search target.
54366	A is SB without orbit, N04: $\Delta RV = 1.6$. A new triple with the physical PSC companion at $11''9$.
56242	Aab is a $0''1$ pair WSI 9107. AB = STF 1547 at $15''$ is physical.
56282	NOMAD: PM(B) = $(0, 500)$, $V(B) = 16.83$ (?). B is physical, PM(A) = $(+43, -158)$. A is SB without orbit, N04: $\Delta RV = 7.4$. This is a new triple system.
56441	NOMAD: PM(B) = $(-164, 0)$, $V(B) = 15.71$ (?). B is physical. PM(A) = $(-92, +1)$.
58180	A is X-ray source RX J1156.0-7700 with small PM(A) = $(-45, +1)$. B at $13''4$ is physical based on CMDs, but the field is crowded, $N^* = 79$.
58240	B = HIP 58241. AB is a known CPM pair DUN 116 at $19''$, 82° . Ba, Bb is a new close pair: $3''6$ 116° , $\Delta K = 5.8$, status unknown.
59021	Both components A, B are above the MS by 1.5 mag. Wrong parallax? The photometric parallax would be ~ 40 mas.
59250	Not observed, but B at $17''$ is possibly physical.
59272	Companion B at $9''3$ is physical, C at $10''7$ is optical.
61298	Not observed, but B at $18''7$ is bright and likely physical, considering that $N^* = 12$.
61608	Not observed, the status of B at $5''5$ is uncertain, could be physical (it is close and bright, $N^* = 11$).
61698	NOMAD: PM(B) = $(-60, +1)$, $V(B) = 11.54$. B is optical. Crowded field, $N^* = 96$. PM(A) = $(-65, -1)$.
62860	A is a ROSAT X-ray source. B at $10''7$ is physical.
62925	B is physical, itself possibly a close binary as hinted by the residuals of the PSF fit. Small PM(A) = $(-33, -40)$. NOMAD: PM(B) = $(+194, +500)$, $V(B) = 16.74$ (??)
63559	A is SB without orbit, N04: $\Delta RV = 17.0$. NOMAD: PM(B) = $(-6, -15)$, $V(B) = 15.64$. B is definitely optical.
64030	HIP 63810 at $2551''$ is CPM, possibly forming a wide triple system with AB = STF 1719 at $7''$.
64459	B at $8''$ is MUG 3 in the WDS, physical. Confirmed by ANDICAM images.
67121	NOMAD: PM(B) = $(-26, -13)$, $V(B) = 11.57$. B is optical. A is SB without orbit (N04: $\Delta RV = 14.8$).
68038	Observed under bad seeing. Small PM(A) = $(+5, +13)$. B at $8''$ is optical.
68507	Linear configuration. The PSC companion B at $6''7$ is physical, but C = SEE 195 at $14''1$ opposite to B is optical. A is SB without orbit (N04: $\Delta RV = 5.4$) and astrometric binary (Hipparcos). This is a new triple system. The visual pair SEE 195 listed in the WDS is optical and corresponds to AC.
69281	Aab is HDS 1989, $0''6$. AC at $24''$ is LDS 1406. The 2MASS companion at $12''6$ is physical.

TABLE 3—*Continued*

HIP	Text
	It is not seen in the V -band images, too red and faint.
	Is this a visual multiple system with 4 components or a small cluster?
70330	NOMAD: PM(B)=(-1,-16), $V(B)=12.17$. B is certainly optical. A is SB without orbit (N04: $\Delta RV=7.6$).
71682	Linear configuration, C is between AB. NOMAD: PM(B)=(+1,+2). B is optical.
72764	Triple physical system BU 31: AB at $1''$ and AC at $8''4$.
72998	NOMAD lists several companions, but B at $18''$, 51° is not found there; B is optical.
73674	AB = HJ 4727 at $7''4$ is physical. No new data for the PSC companion C at $11''2$, it is likely optical (crowded field, $N^*=38$).
74888	The companion B is barely seen in the 30-s V -band image, it is physical. No references in SIMBAD.
74930	B = HIP 74931. AB = STF 1931 at $13''3$ is physical.
75790	AB is the $0''8$ pair BU 1114, the PSC companion at $10''$ is HJ 4774, physical (designated C in the WDS).
76572	NOMAD lists several components within $20''$, but none matches B. Crowded field, $N^*=32$. B at $14''2$, 314° is optical. A is listed in the WDS as a $3''8$ pair HDS 2206, but this companion is definitely not present in the ANDICAM images.
76603	B = HIP 76602. AB = STF 1962 at $11''8$ is physical.
77203	Small PM(A)=(-49,-13). NOMAD: PM(B)=(+58,-28), $V(B)=13.35$. B is optical.
78738	B = HIP 78739. AB = STF 1999 at $11''9$ is physical.
79048	The 2MASS companion at $10''3$, 356° is likely an artifact, in which case another companion at $7''6$ in ANDICAM images is measured.
79143	NOMAD: PM(B)=(-4,-9). B is optical. PM(A)=(-9,-24). Crowded field, $N^*=100$.
79169	Another companion C at $5''42$ 337° , $\Delta K=5.41$ is seen in the ANDICAM K - and V -band images. Crowded field, $N^*=40$.
81274	NOMAD: PM(B)=(-51,+56), $V(B)=14.47$. B is physical. PM(A)=(-29,+49).
82384	Small PM(A)=(-1,+26). NOMAD: PM(B)=(-6,-38). B remains of uncertain status.
83083	NOMAD: PM(B)=(+17,+14), $V(B)=16.21$. B is optical. PM(A)=(-24,+141).
84866	Aab is a visual binary A 953 with $P=73.5y$ and $a=0''262$. The PSC companion B at $10''1$ is physical. A new triple system.
85141	Aab = RST3972, $0''1$, orbit $P=15y$. NOMAD: PM(B)=(-3,+2), $V=15.71$. B is optical.
85307	A = HR 6489, F3V, PM(A)=(+61,+52). NOMAD: PM(B)=(-62,+75). The status of B is uncertain, it is not found in the WDS. A,B are ~ 1 mag above the MS (true parallax $25mas?$). Nothing on B in SIMBAD. Crowded field, $N^*=73$.

TABLE 4
COMPANION COUNT

J_{abs}	n_p	n_o	n_c	α	q_0
6-7	61	20	51 ± 8	0.84	0.51
7-8	45	27	31 ± 7	0.70	0.34
8-9	41	51	15 ± 7	0.38	0.19
9-10	59	107	5 ± 9	0.09	0.12